**MTS Lecture -- American Rock Mechanics Association**

49th U .S. Rock Mechanics / Geomechanics Symposium

28 June - 1 July, 2015, San Francisco, CA

# *Thermo-Poro-Mechanics of Strain Localization in Rapidly Sheared Granular Rock, and Implications for Earthquake Source Physics*

**James R. Rice** (Harvard)

***Underlying studies done collaboratively with some of:***

**Nicolas Brantut** (Univ Col Lond)
**Massimo Cocco** (INGV Rome)
**Eric Dunham** (Stanford Univ)
**Nadia Lapusta** (Caltech)
**Hiroyuki Noda** (JAMSTEC)
**John Platt** (Carnegie Inst Wash)
**Alan Rempel** (Univ Oregon)
**John Rudnicki** (Northwestern)

***Quandary in seismology:***

**• Lab (J. Byerlee et al.) and field (M. D. Zoback et al.) estimates of friction coefficient are usually high, $f$ ~ 0.6-0.8.**

**Shear strength $\tau = f \times (\sigma_n - p)$, where:**

**$\sigma_n$ = normal stress clamping the fault shut**
**$p$ = pore pressure in infiltrating fluid phase**

**• Fault slip zones are thin (despite wide damage zones of 1-$10^3$ m).**

**==> If those $f$ prevail during seismic slip, and $p$ ~ hydrostatic, we should find**

- ***measurable heat outflow*** **near major faults, and/or**
- ***extensive melt*** **signatures along exhumed faults.**

**Neither effect is <u>generally</u> found.**

Chester & Chester

[*Tectonophys.*, 1998]

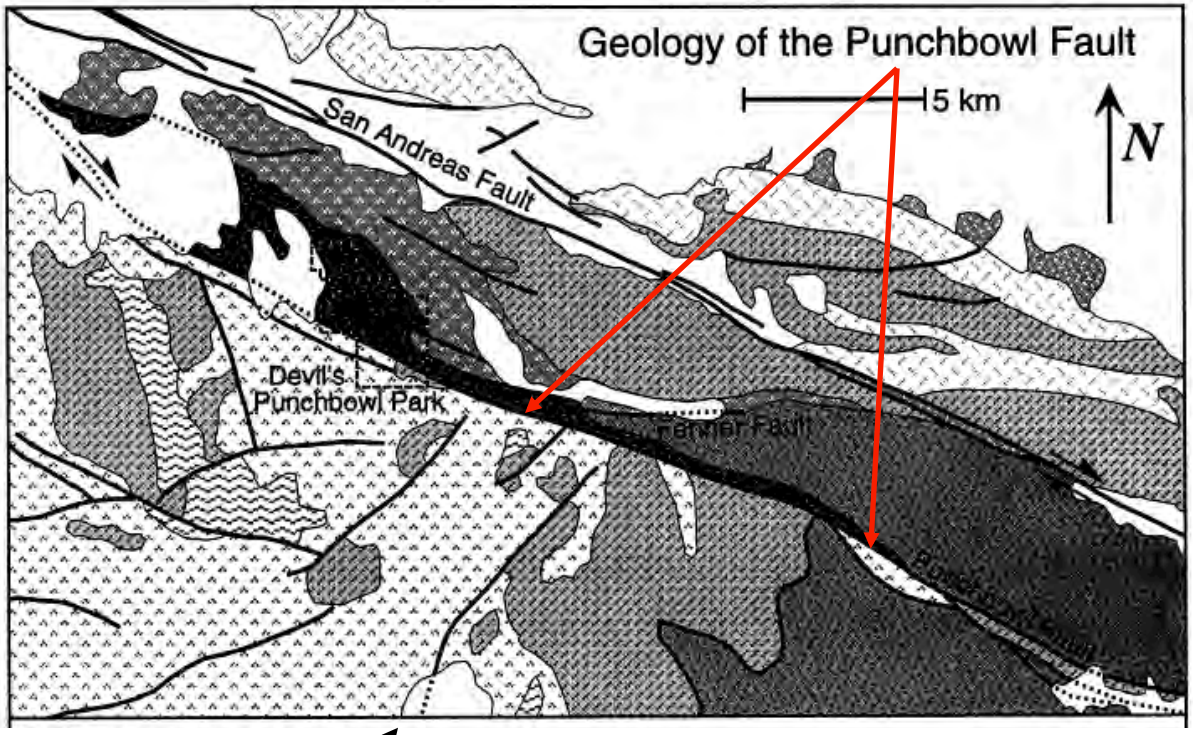


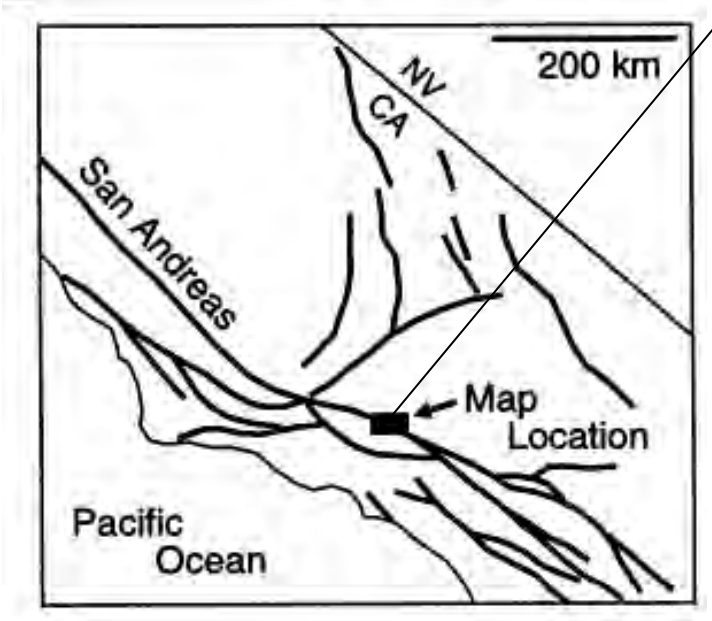


# Earthquake shear is highly localized!

Punchbowl PSS, composite based on Chester & Chester [*Tectonophys* ‘98] & Chester & Goldsby [*SCEC* ‘03]

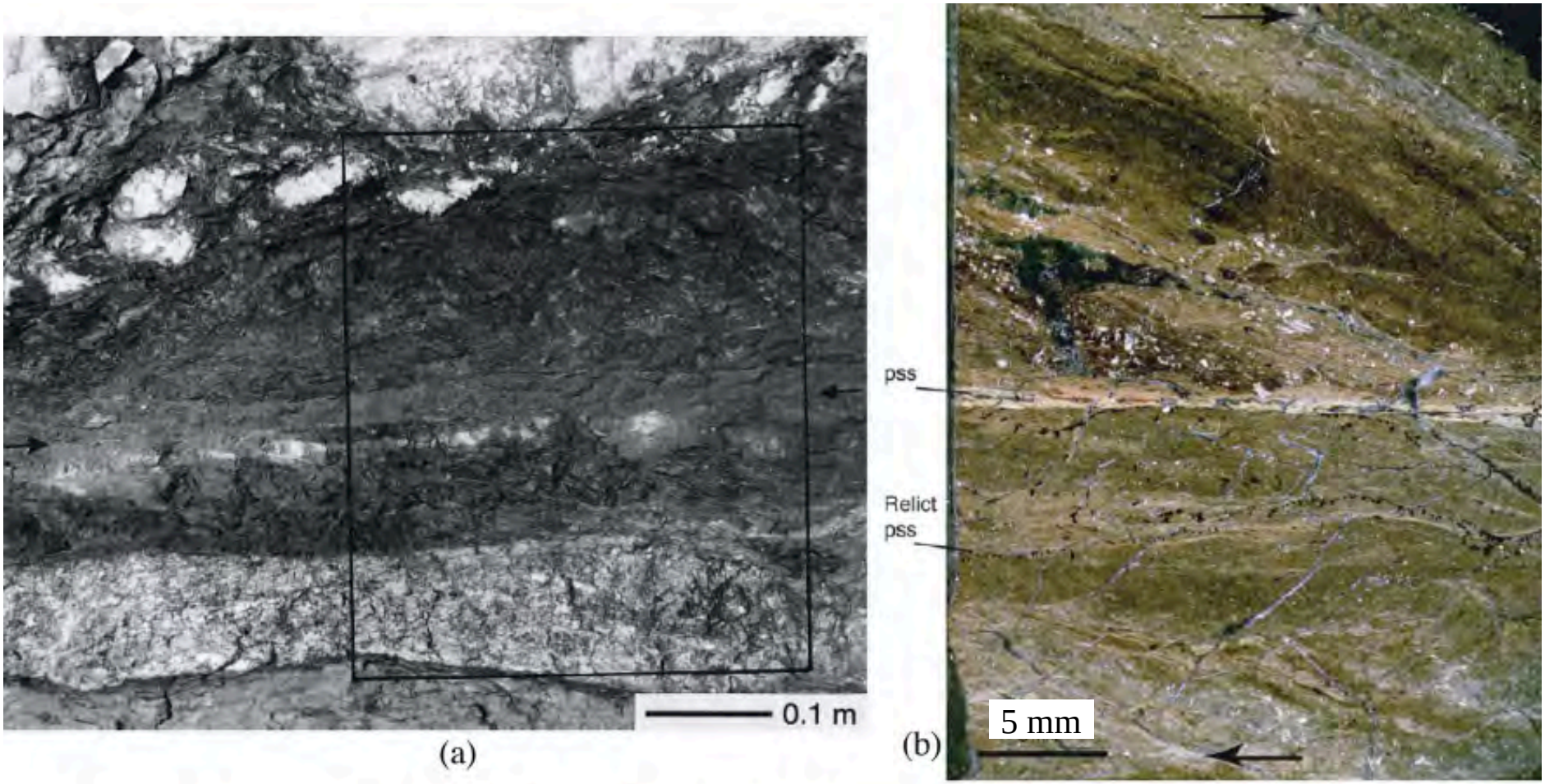


**Figure 1.** Principal slip surface (PSS) along the Punchbowl fault. (a) From *Chester and Chester* [1998]: Ultracataclasite zone with PSS marked by black arrows; note 100 mm scale bar. (b) From Chester et al. (manuscript in preparation, 2005) [also *Chester et al.*, 2003; *Chester and Goldsby*, 2003]: Thin section; note 5 mm scale bar and ~1 mm localization zone (bright strip when viewed in crossed polarizers due to preferred orientation), with microshear localization of most intense straining to ~100–300 μm thickness.

[Heermance, Shipton & Evans, *BSSA*, 2003]

***Core retrieved across the Chelungpu fault, which hosted the 1999 Mw 7.6 Chi-Chi, Taiwan, earthquake:*** **Suggests slip at 328 m depth traverse was accommodated within a zone ~ 50–300 μm thick.**

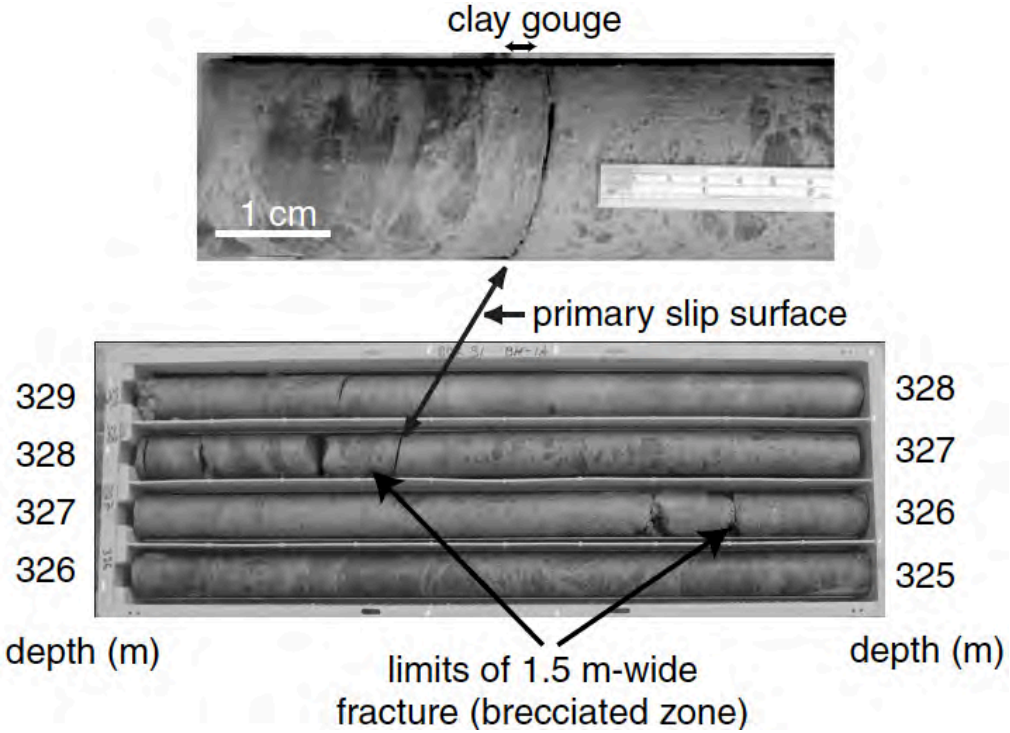


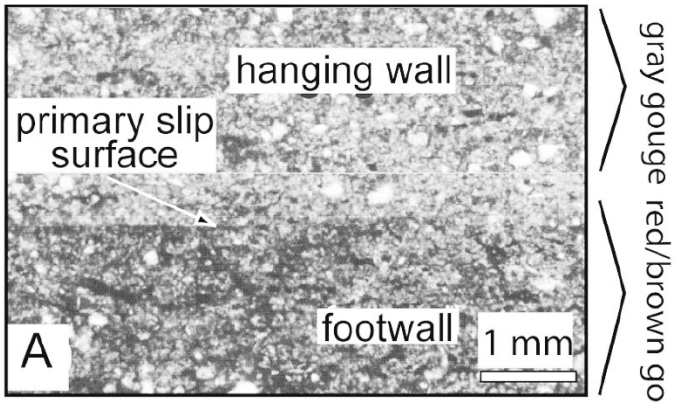


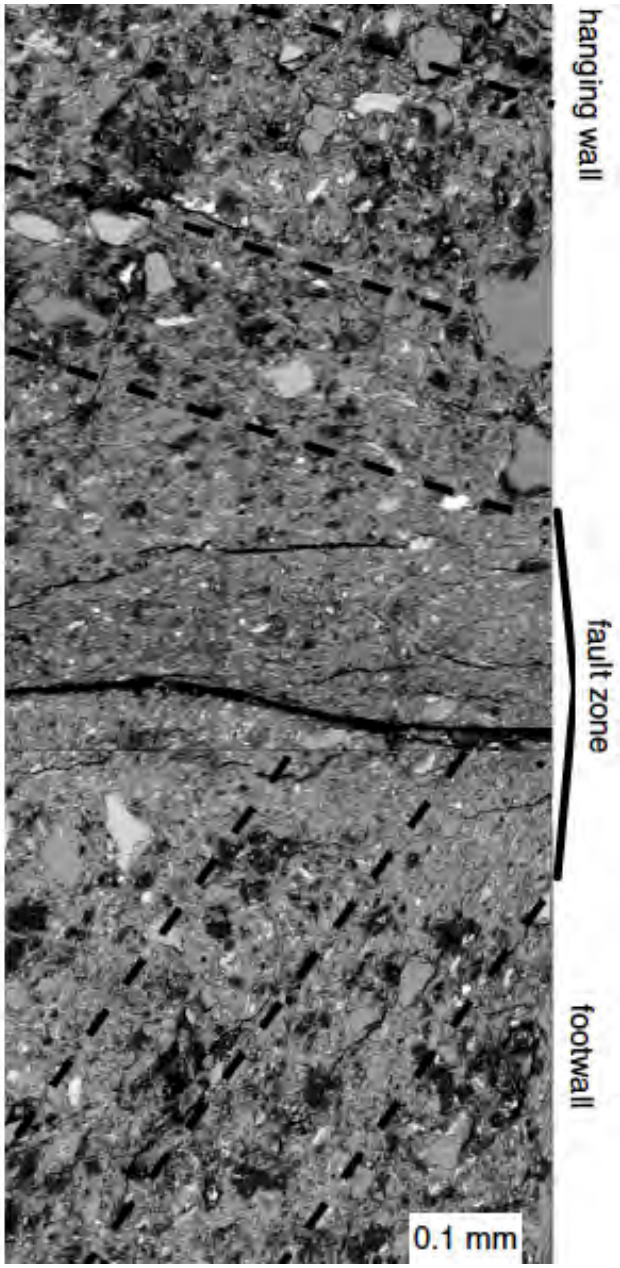

***Two other Chelungpu Fault,Taiwan boreholes***
[Boullier et al., GGG 2009, GSL 2011]:
**Principal Slip Zone (PSZ) localized within black gouges**

**• Hole A, fault at 1111 m depth: PSZ is ~2 cm thick**

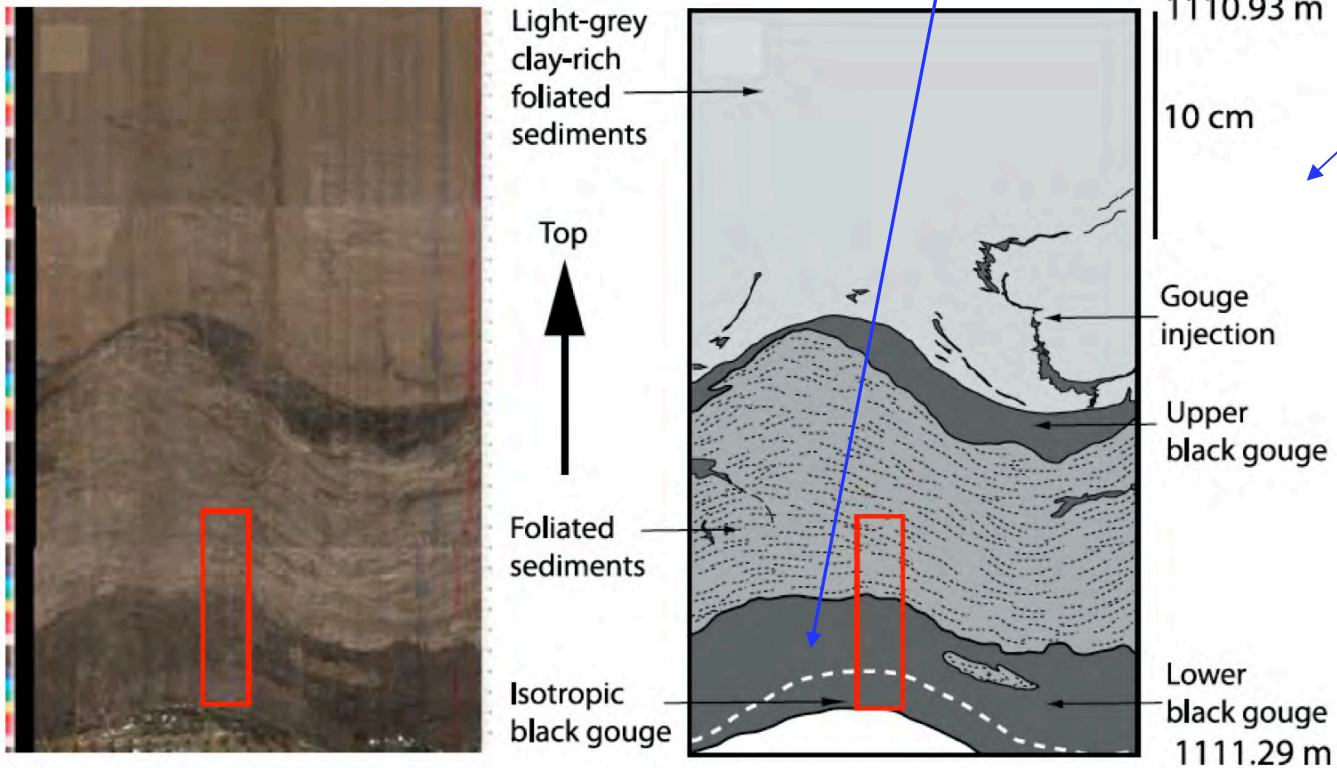


Unrolled scanning image of FZA1111 and corresponding sketch

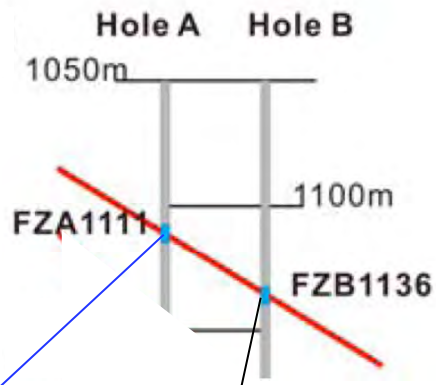


A

B

**• Hole B, fault at 1136 m depth: PSZ is ~3 mm thick**

PSZ layering defined by variations in concentrations of clay minerals and clasts, comparable to structures produced in high-rate rotary shear exp's.

**Median Tectonic Line Fault, Japan**



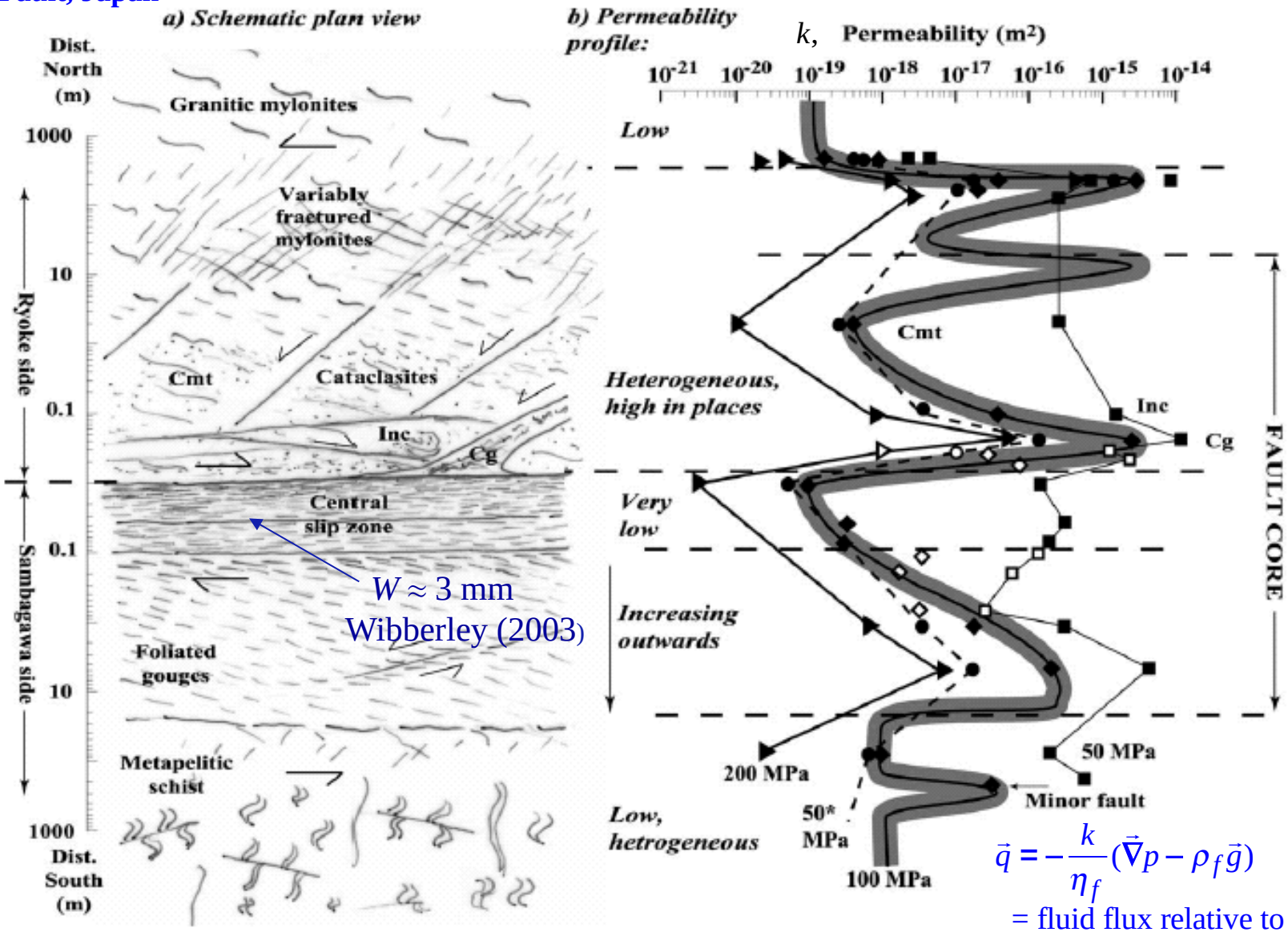


$$\vec{q} = -\frac{k}{\eta_f}(\vec{\nabla}p - \rho_f \vec{g})$$

= fluid flux relative to solid host

***This study:*** Primary source of data we use for gouge ***porosity***, ***compressibility*** and ***permeability*** as functions of effective confining stress (and its history).

$$\tau = f \times (\sigma_n - p)$$

***Statically strong but dynamically weak faults, e.g., due to thermal weakening in rapid, large slip:***

- ***Process expected to be important from start of seismic slip:***

**- Thermal pressurization of in-situ pore fluid, reduces effective stress.**

- ***Process that may set in at large enough rise in T*:**

**- Thermal decomposition, fluid product phase at high pressure (*e.g.*, $CO_2$ from carbonates; $H_2O$ from clays or serpentines).**

- ***Ultimately:***

**- Melting at large slip, *if* above have not limited increase of *T*.**

# Shear of a fluid-saturated gouge layer

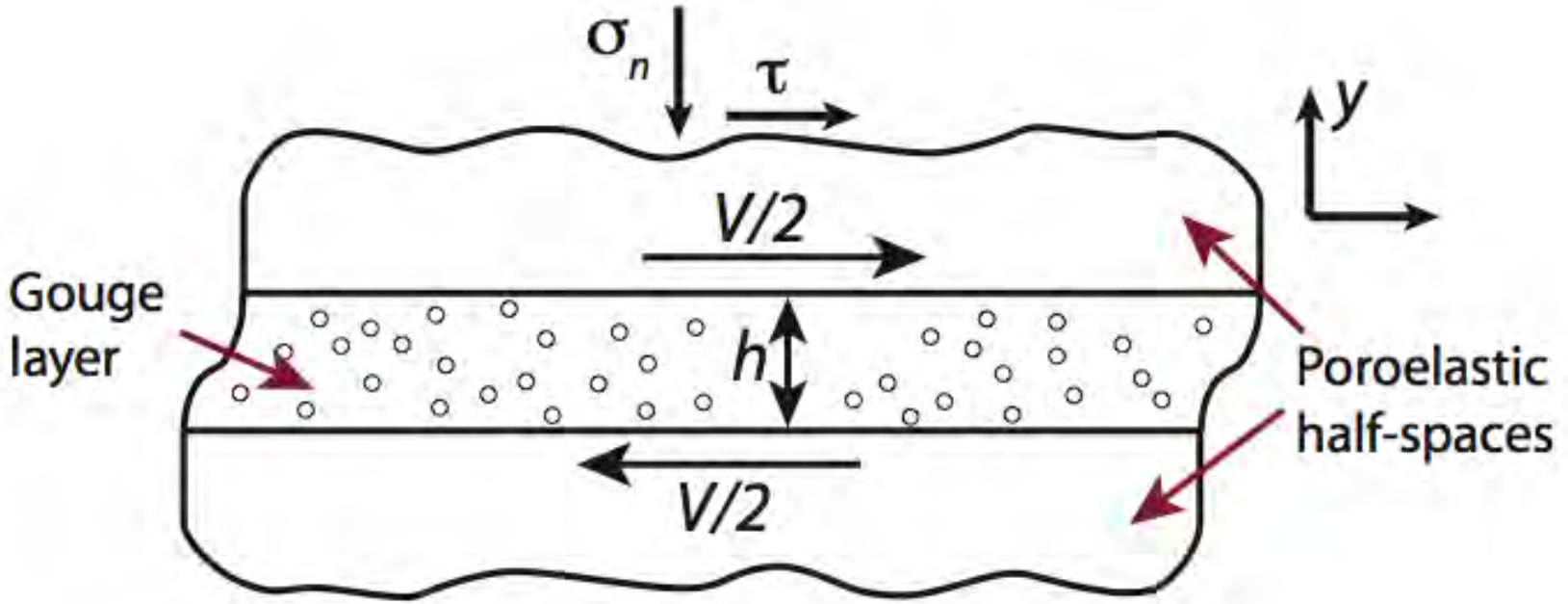


- Two non-yielding half-spaces are moved relative to each other at a speed $V$ (typically, $V$ ~ 1 m/s).
- All inelastic deformation accommodated in gouge layer, leading to a nominal strain rate $\dot{\gamma}_0 = V / h$ .

Rice, Rudnicki & Platt (JGR 2014) –- formulation analogous to Benallal (CR Mec 2005)

# Thermo-mechanical model in gouge layer

- To model the deforming gouge layer we use,

Mechanical equilibrium $$\frac{\partial \tau}{\partial y} = 0, \quad \frac{\partial \sigma_n}{\partial y} = 0$$

Conservation of energy $$\frac{\partial T}{\partial t} - \alpha_{th} \frac{\partial^2 T}{\partial y^2} = \frac{\tau \dot{\gamma}}{\rho c}$$

Conservation of fluid mass $$\frac{\partial p}{\partial t} - \alpha_{hy} \frac{\partial^2 p}{\partial y^2} = \Lambda \frac{\partial T}{\partial t}$$

- Shear stress modeled using the effective stress and ***rate-strengthening*** friction,

$$\tau = f(\dot{\gamma})(\sigma_n - p) \qquad f(\dot{\gamma}) = f_0 + (a-b)\log\left(\frac{\dot{\gamma}}{\dot{\gamma}_0}\right)$$

$$\left(\text{We assume } a - b \equiv \left(\dot{\gamma} df(\dot{\gamma}) / d\dot{\gamma}\right)_{\dot{\gamma}=\dot{\gamma}_0} > 0\right)$$

**Shear between moving rigid blocks of perfectly insulating, impermeable material :**

**Exact homogeneous shear solution (Lachenbruch, JGR, 1980, version ignoring dilatancy) :**

$$\tau(t) = f_o\left(\sigma_n - p(t)\right) = f_o\left(\sigma_n - p_a\right)\exp\left(-f_o\frac{\Lambda}{\rho c}\frac{Vt}{h}\right),$$

$$\left(\textit{Exponential decay of strength with slip}\right)$$

## Linearized perturbation analysis :

**Is that solution stable to small perturbations?**

***Not unless h is very small* !**

Stable only if $h \le W_{crit} \equiv \dfrac{\pi^2}{\left(2+\dfrac{f_o}{a-b}\right)}\dfrac{\rho c}{f_o\Lambda}\dfrac{\left(\alpha_{th}+\alpha_{hy}\right)}{V}.$

$$\left(\text{Typically, } \frac{f_o}{a-b} >> 2 \Rightarrow W_{crit} \approx \pi^2\frac{a-b}{f_o^2}\frac{\rho c}{\Lambda}\frac{\alpha_{th}+\alpha_{hy}}{V}\ .\right)$$

[$W_{crit} = \lambda_{shr}/2$, where $\lambda_{shr}$ = longest wavelenth $\lambda$ for stable linearized response to infinitesimal $\exp(2\pi iy/\lambda)$ perturbation]

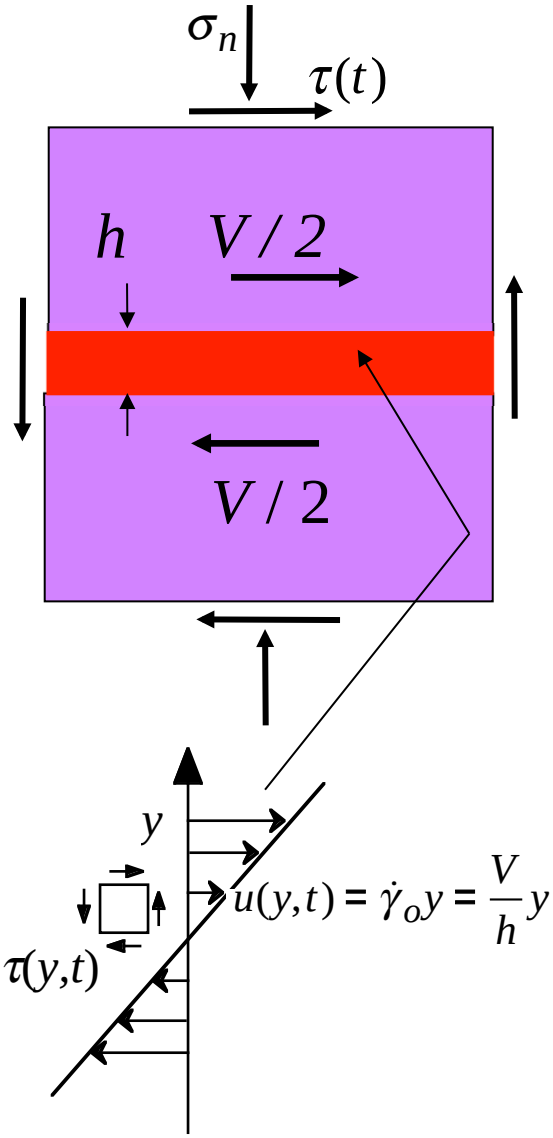


Rice, Rudnicki & Platt (JGR 2014)

***Estimates of maximum stable shear layer thickness (i.e., localized zone width)*** $W_{crit}$

*Results*, using $f_o = 0.4$, $\dfrac{f_o}{a-b} = 20$, $V = 1\ \dfrac{\text{m}}{\text{s}}$, $\alpha_{th} = 0.7\ \dfrac{\text{mm}^2}{\text{s}}$, $\rho c = 2.7\ \dfrac{\text{MPa}}{^o\text{C}}$ :

**Corresponding to ~ 7 km depth :**

***Low estimate*** (Based on lab properties of ***intact*** Median Tectonic Line gouge [Wibberley and Shimamoto, 2003] at effective confining stress = 125 MPa and $T$ = 200ºC):

$$\Lambda = 0.70\ \frac{\text{MPa}}{^o\text{C}}, \quad \text{and} \quad \alpha_{hy} = 1.5\ \frac{\text{mm}^2}{\text{s}} \quad \Rightarrow \quad \boxed{W_{crit} = \text{3-5 } \mu\text{m}}$$

***High estimate*** (Accounts very roughly for ***fresh damage*** of the initially intact fault gouge, introduced at the rupture front just before and during shear, by increasing permeability $k$ to $k^{dmg}$ = 5-10 $k$, and increasing drained compressibility $\beta_d$ to $\beta_d^{dmg}$ = 1.5-2 $\beta_d$ ):

$$\Lambda \approx 0.34\ \frac{\text{MPa}}{^o\text{C}}, \quad \text{and} \quad \alpha_{hy} \approx 3.5\ \frac{\text{mm}^2}{\text{s}} \quad \Rightarrow \quad \boxed{W_{crit} \approx \text{25-40 } \mu\text{m}}$$

**Corresponding to ~ 1 km depth :**

***Low estimate :*** $\boxed{W_{crit} \sim 25\ \mu\text{m}}$ ***High estimate :*** $\boxed{W_{crit} \sim 200\ \mu\text{m}}$

Rice, Rudnicki & Platt (JGR 2014)

## *Now: Full nonlinear numerical solution results*

[Platt, Rudnicki, and Rice, JGR 2014]

Shear of a fluid-saturated gouge layer

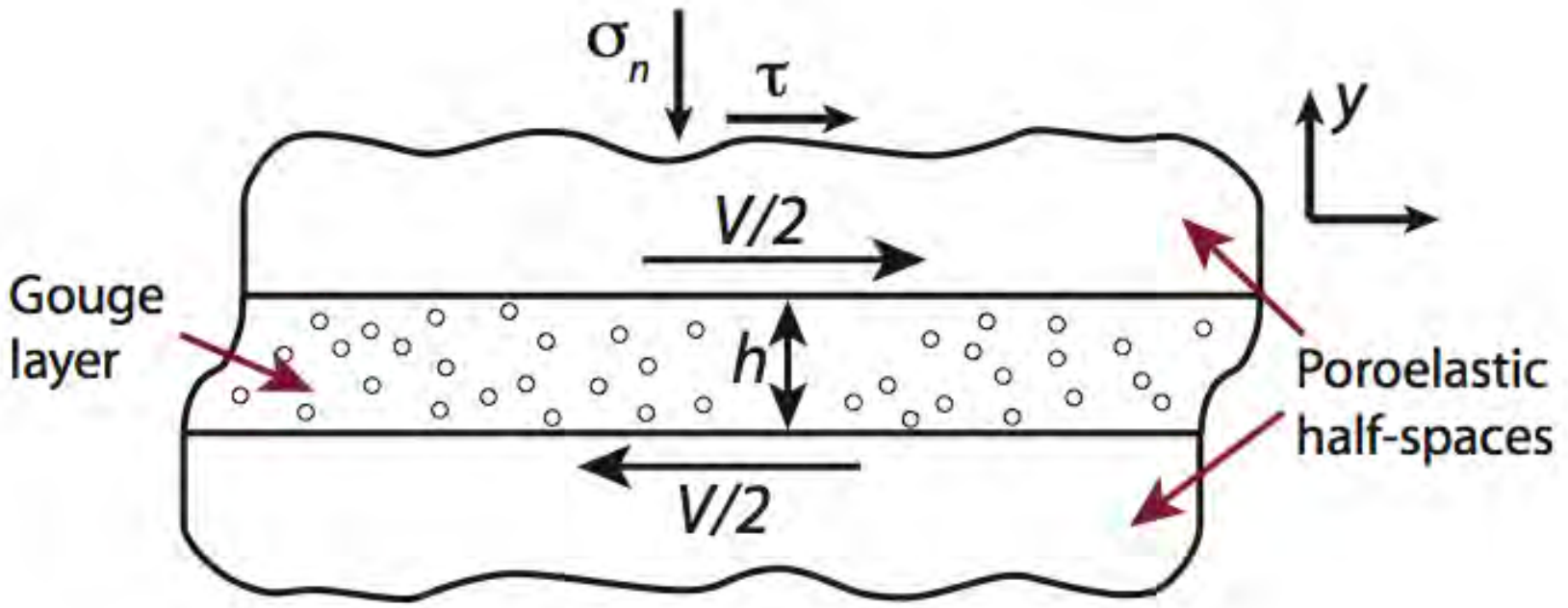


- Two non-yielding half-spaces are moved relative to each other at a speed $V$ (typically, $V$ ~ 1 m/s).
- All inelastic deformation accommodated in gouge layer, leading to a nominal strain rate $\dot{\gamma}_0 = V / h$ .

Platt, Rudnicki, and Rice (JGR 2014)

# Strain localization

**• Full nonlinear numerical simulations (vs. linear perturbations), using representative physical values predict that strain localization does occur.**

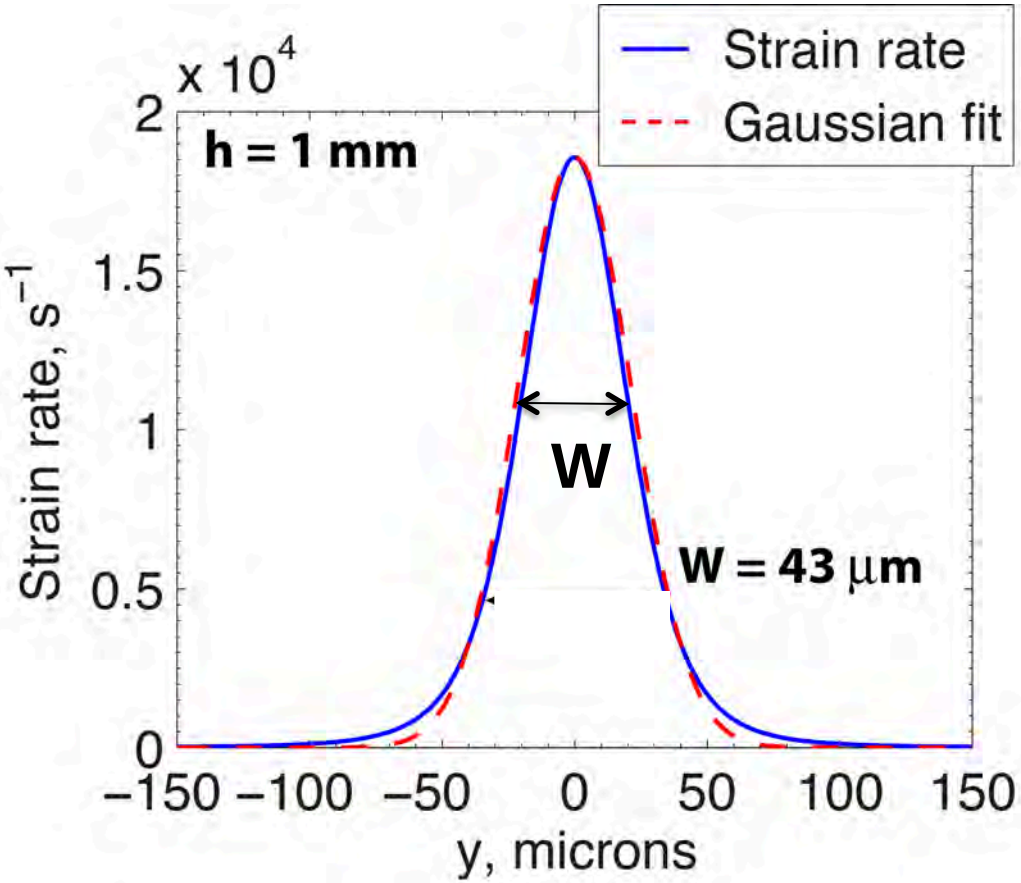


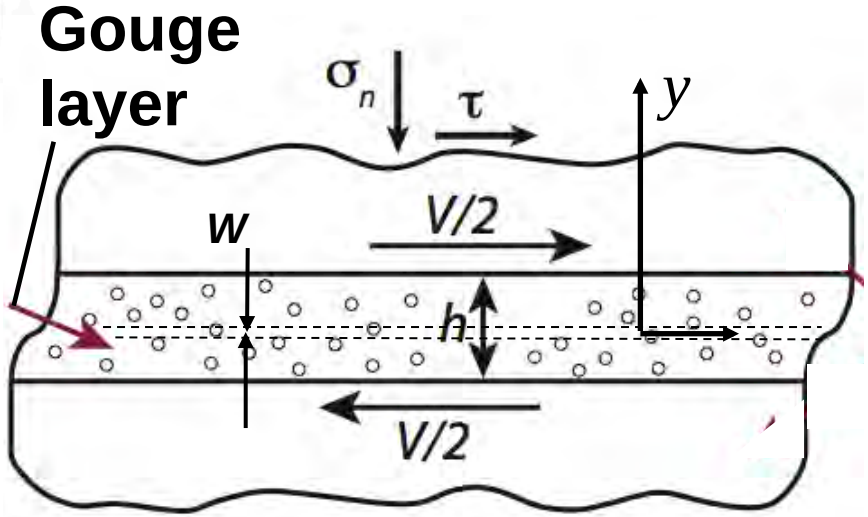


• Deformation has localized to a zone much thinner than the layer, $W << h$ (43 μm << 1,000 μm).

$W_{\text{nonlin. calc.}}$ is comparable to $W_{\text{lin. pert.}}$ .

# Implications, dynamic weakening

Platt, Rudnicki & Rice (JGR 2014)

- Weakening of a gouge layer during localization

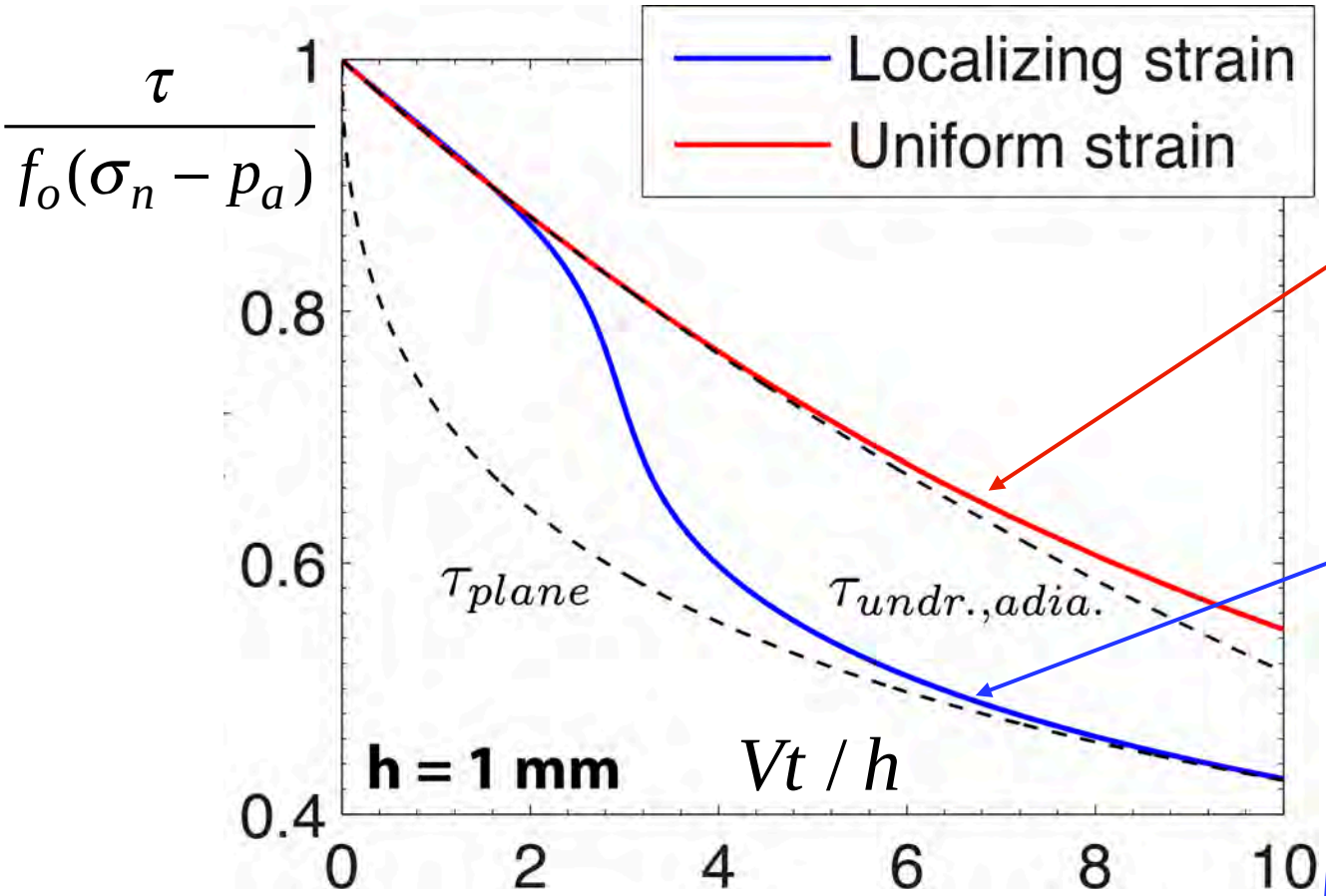


Closely follows Lachenbruch [*JGR*,1980] sol'n (Here, transport at boundary allowed).

Closely follows "slip on a plane" Rice [*JGR*, 2006] sol'n, generalizing Mase & Smith [*JGR*,1987] sol'n.

- Localization leads to additional weakening.

$$\tau = f_o(\sigma_n - p_a)\exp\left(\frac{Vt}{L^*}\right)\mathrm{erfc}\left(\sqrt{\frac{Vt}{L^*}}\right) \quad \text{where} \quad L^* = \left(\frac{2\rho c}{f_o\Lambda}\right)^2 \frac{\left(\sqrt{\alpha_{hy}} + \sqrt{\alpha_{th}}\right)^2}{V}$$

$$\tau = f \times (\sigma_n - p)$$

***Statically strong but dynamically weak faults, e.g., due to thermal weakening in rapid, large slip:***

- ***Process expected to be important from start of seismic slip:***

**- Thermal pressurization of in-situ pore fluid, reduces effective stress.**

- ***Process that may set in at large enough rise in T*:**

**- Thermal decomposition, fluid product phase at high pressure (*e.g.*, $CO_2$ from carbonates; $H_2O$ from clays or serpentines).**

- ***Ultimately:***

**- Melting at large slip, *if* above have not limited increase of *T*.**

***Examples, thermal decomposition:***

***Dolomite***, **$CaMg(CO_3)_2$** (De Paola et al., *Tectonics*, 2008, *Geology*, 2011; Goren et al., *J. Geophys. Res.*, 2010):

- At *T* ~ 550ºC, dolomite decomposes to calcite, periclase, and carbon dioxide:

$$CaMg(CO_3)_2 \rightarrow CaCO_3 + MgO + CO_2$$

- At *T* ~ 700-900ºC, the calcite further decomposes to lime and carbon dioxide:

$$CaCO_3 \rightarrow CaO + CO_2$$

***Many clays and hydrous silicates*** (Brantut et al., *J. Geophys. Res.*, 2010):

- At *T* ~ 500ºC (~300ºC for smectite, ~ 800ºC for chlorite), decomposition releasing $H_2O$ starts.

***Gypsum***, **$CaSO_4(H_2O)_2$)** (Brantut et al., *Geology*, 2010):

- At *T* ~ 100ºC, gypsum dehydrates to form bassanite:

$$CaSO_4(H_2O)_2 \rightarrow CaSO_4(H_2O)_{0.5} + 1.5\ H_2O$$

- At *T* ~ 140ºC, bassanite turns into anhydrite

$$CaS_4(H_2O)0.5 \rightarrow CaSO_4 + 0.5\ H_2O$$

# Example, recent version of Toshi Shimamoto's rotary shear apparatus (at Instititute of Geology, Peking University)



a

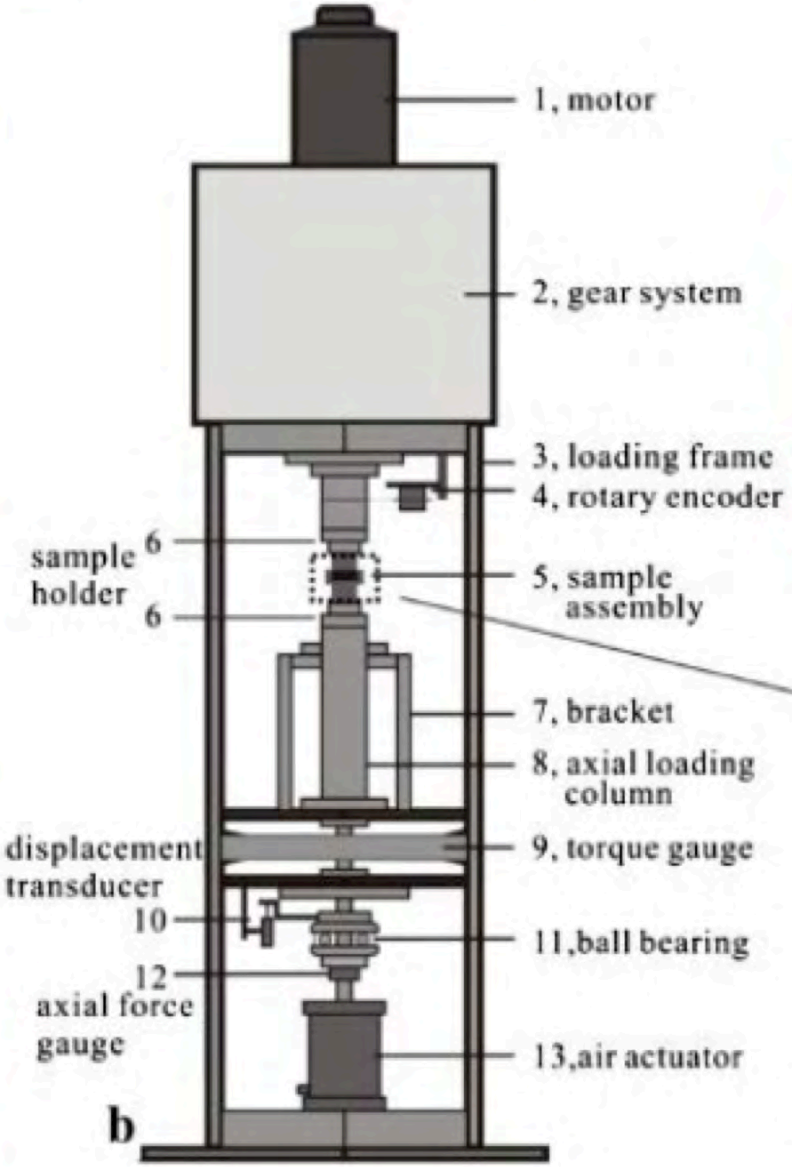


b

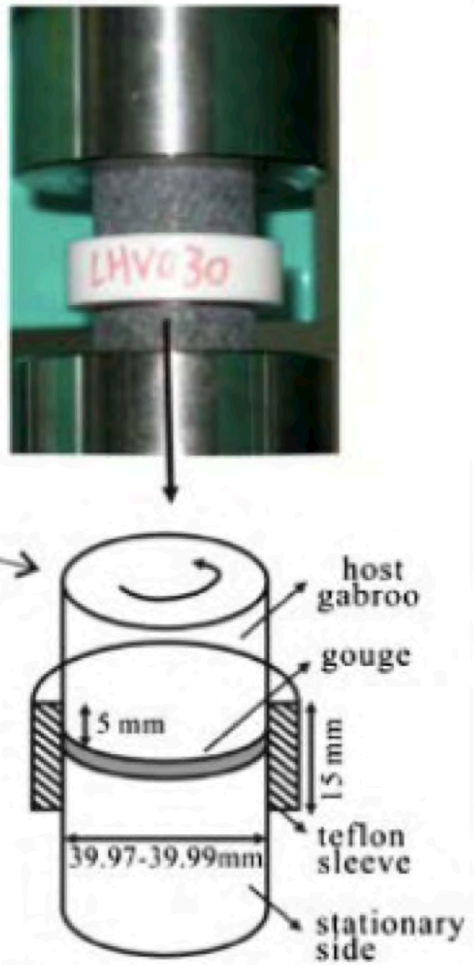


c

[Han, Shimamoto, Hirose, Ree & Ando, *Sci.,* 2007]:

***Carbonate Faults***

Simulated faults in Carrara Marble at subseismic to seismic slip rates

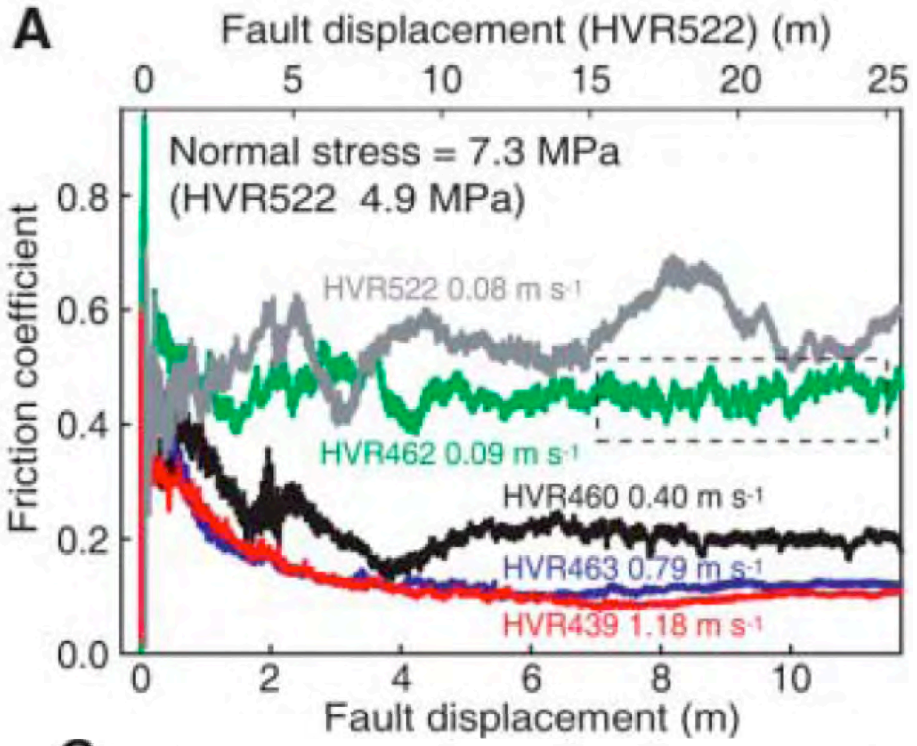


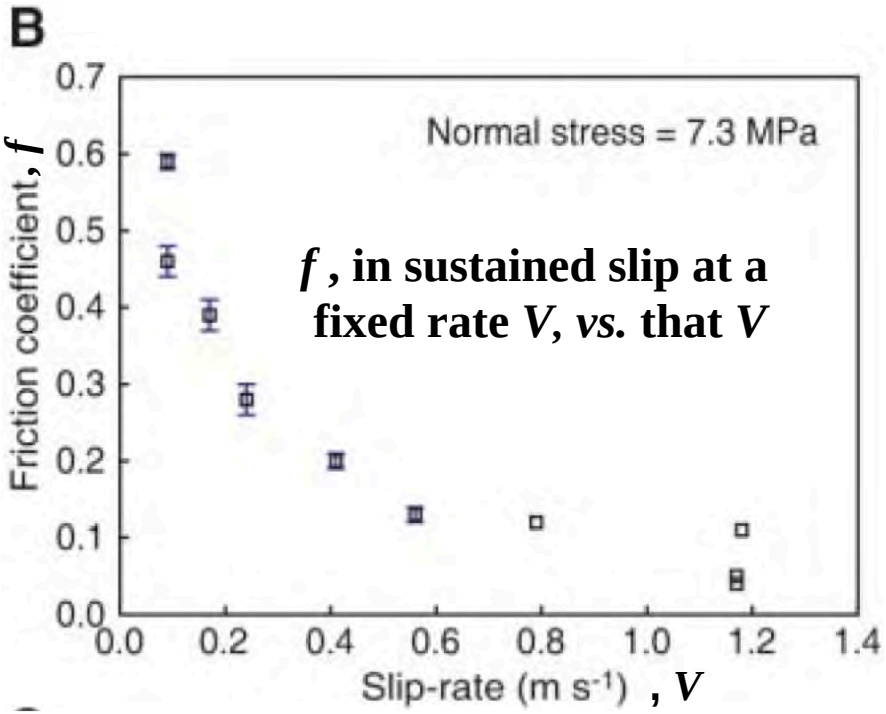


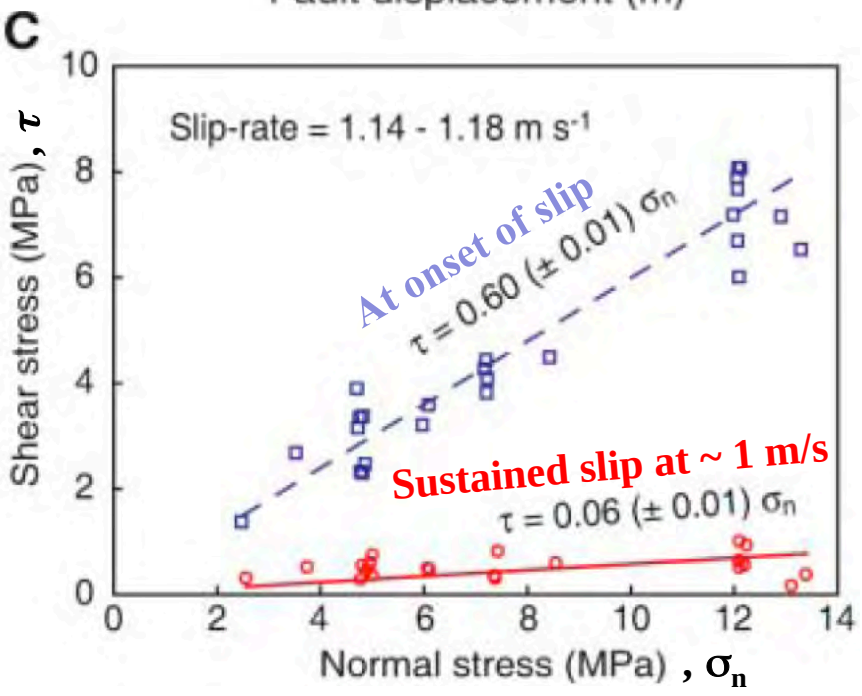

# Model for decomposing gouge material

- To model the deforming gouge layer we use, based on J. Sulem, I. Vardoulakis, and co-workers (Brantut, Ghabezloo, Famin, Lazar, Noda, Schubnel, Stefanou, Veveakis, …),

$$\frac{\partial T}{\partial t} = \frac{\tau\dot{\gamma}}{\rho c} + \alpha_{th}\frac{\partial^2 T}{\partial y^2} - E_r\frac{\partial \xi}{\partial t}$$

$$\frac{\partial p}{\partial t} = \Lambda\frac{\partial T}{\partial t} + \alpha_{hy}\frac{\partial^2 p}{\partial y^2} + P_r\frac{\partial \xi}{\partial t}$$

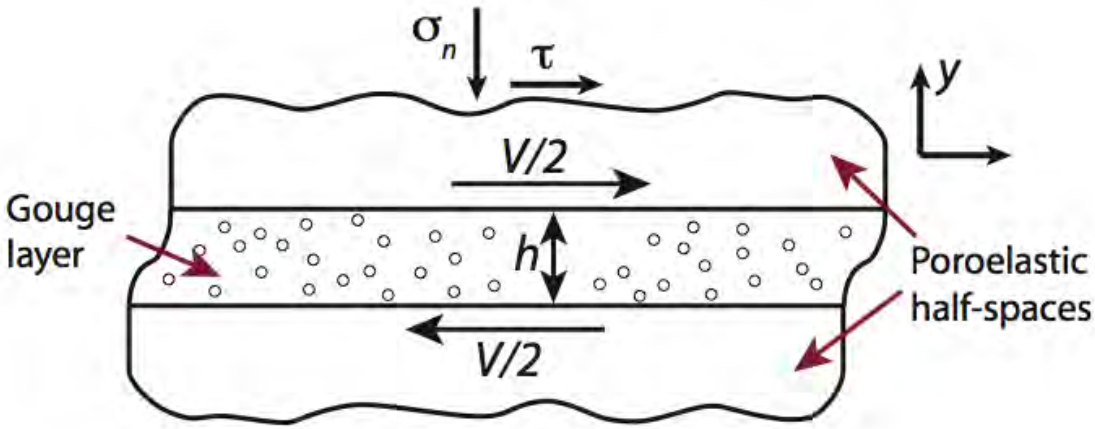


- We assume that the reaction follows an Arrhenius kinetic law,

$$\frac{\partial \xi}{\partial t} = A(1-\xi)\exp\left(-\frac{Q}{RT}\right)$$

**Platt, Brantut & Rice (*JGR*, 2015)**

**Table 2.** List of reaction parameters.

Platt, Brantut & Rice (*JGR*, 2015)

| Parameter | Decarbonation reaction | Dehydration reactions | | |
|---|---|---|---|---|
| | Calcite[a] | Lizardite[b] | Illite/muscovite[c] | Talc[d] |
| Pre-exponential factor, $\log_{10}(A)$ ($A$ in 1/s) | 15.47 | 17.80 | 6.92 | 14.30 |
| Activation energy, $Q$ (kJ/mol) | 319 | 328 | 152 | 372 |
| Fluid mass, $m_{tot}^{100\%}$ (kg/m$^3$), | 1140 | 240 | 150 | 131 |
| Enthalpy[e], $\Delta H$ (MJ/kg) | 7.25 | 2.56 | 5.49 | 5.17 |
| Solid volume change, $\phi$ ($\times 10^{-3}$ m$^3$/kg) | 0.46 | 0.88 | 0.35 | 0.78 |
| Fluid density, $\rho_f$ ( m$^3$/kg) | 418 | 267 | 135 | 159 |
| $T_r$ | 960 °C | 885 °C | 1733 °C | 1454 °C |
| $E_r$ (°C) | $3.06 \times 10^3$ | 275 | 305 | 251 |
| $P_r$ (GPa) | 7.42 | 2.80 | 3.56 | 2.43 |
| $W^{HT}$ | 5.1 $\mu$m | 1.2 $\mu$m | 1.1 $\mu$m | 1.3 $\mu$m |
| $W$ | 12.7 $\mu$m | 6.8 $\mu$m | 11.9 $\mu$m | 8.6 $\mu$m |

***Linear perturbation results*: *very rough estimates of localization zone widths :***

High $T$, fast reaction rate limit: $W^{HT} \approx \pi^2 \dfrac{\alpha_{hy}}{V} \dfrac{(a-b)}{f_o^2} \dfrac{\rho c E_r}{P_r}$

Low $T$, pre-reaction thermal press.: $W \approx \pi^2 \dfrac{a-b}{f_o^2} \dfrac{\rho c}{\Lambda} \dfrac{\alpha_{th}+\alpha_{hy}}{V}$

[$W = \lambda/2$, where $\lambda =$ longest wavelenth for stable linearized response to infinitesimal $\exp(2\pi i y/\lambda)$ perturbation]

Representative simulations:
thermal pressurization of in-situ fluids,
followed by thermal decomposition

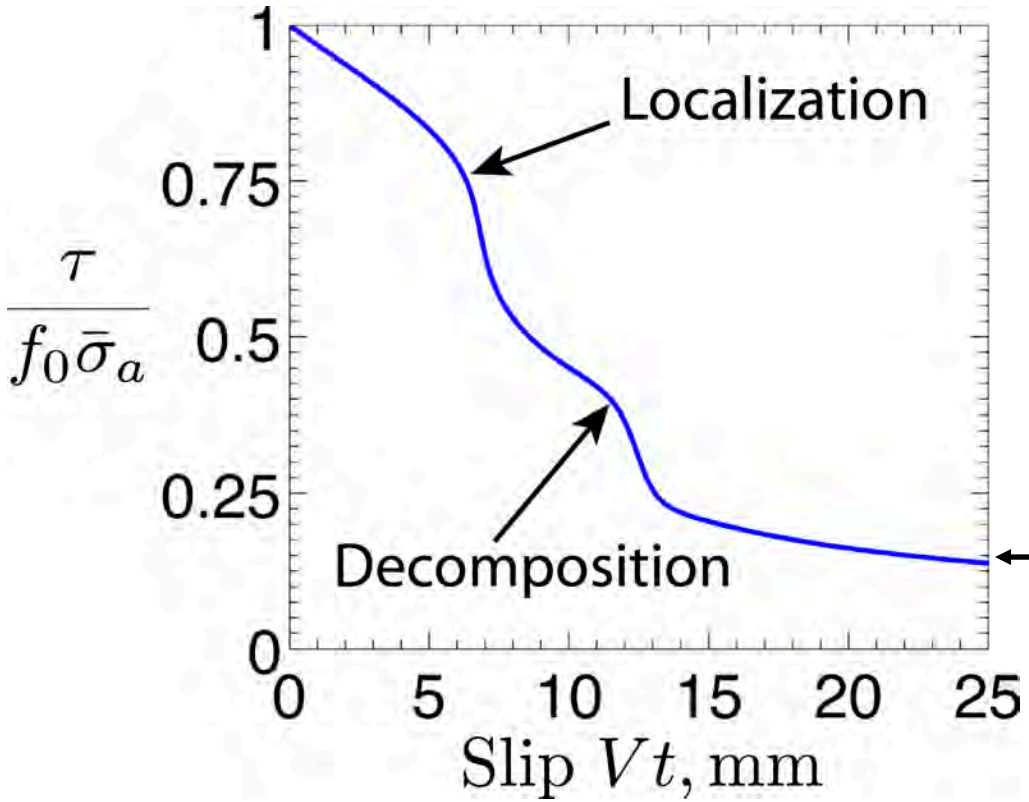


~ 14% of initial friction strength after 25 mm slip

**Supports concept that faults may be *strong* but *brittle***
**(quickly lose strength after slip is initiated at a place of localized stress concentration)**

Platt, Brantut & Rice (AGU, Fall 2011)

- Numerical solutions for a 1 mm wide gouge layer.

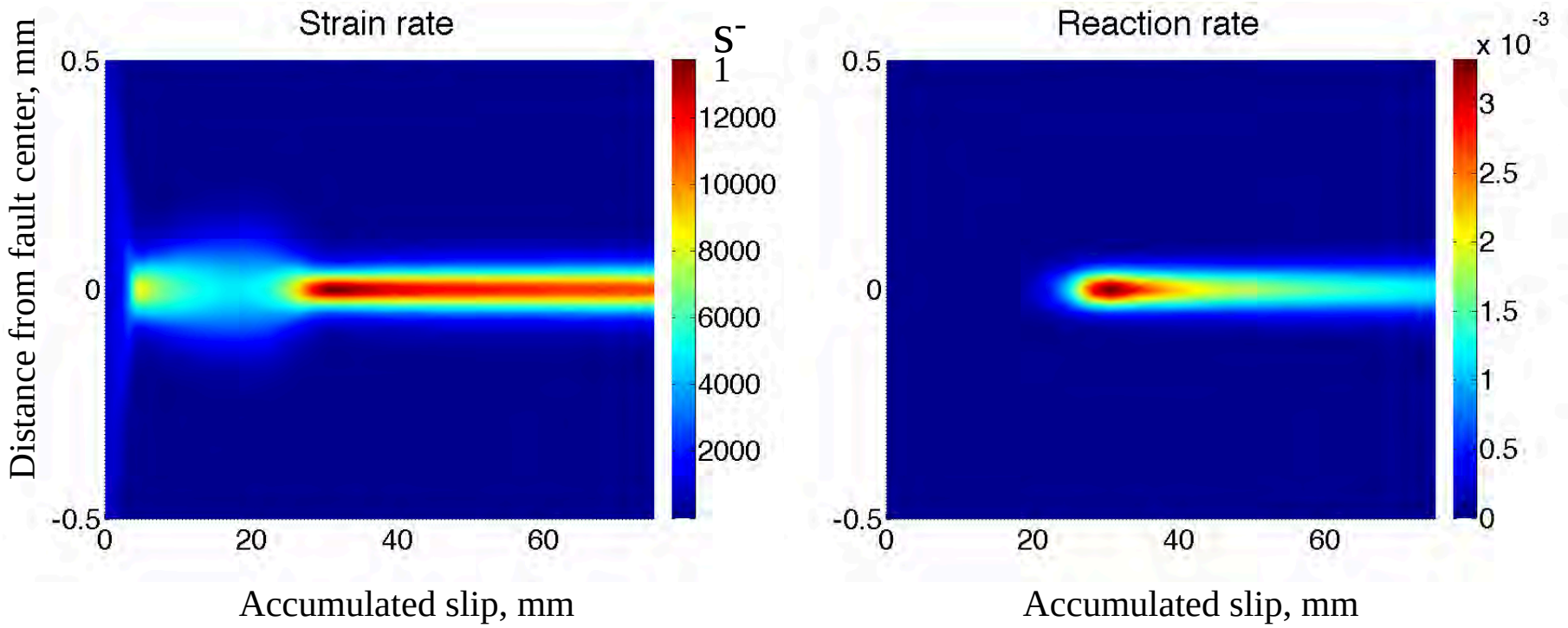


- When the reaction becomes important, we observe significant strain localization ($W_{\text{nonlin. calc.}}$ of order ~ 2 x $W_{\text{lin. pert.}}$ ).

# Independence of reaction rate

• Our linear stability analysis predicts the localized zone width is independent of kinetic parameters. To test this we **increase *A* by three orders of magnitude.**

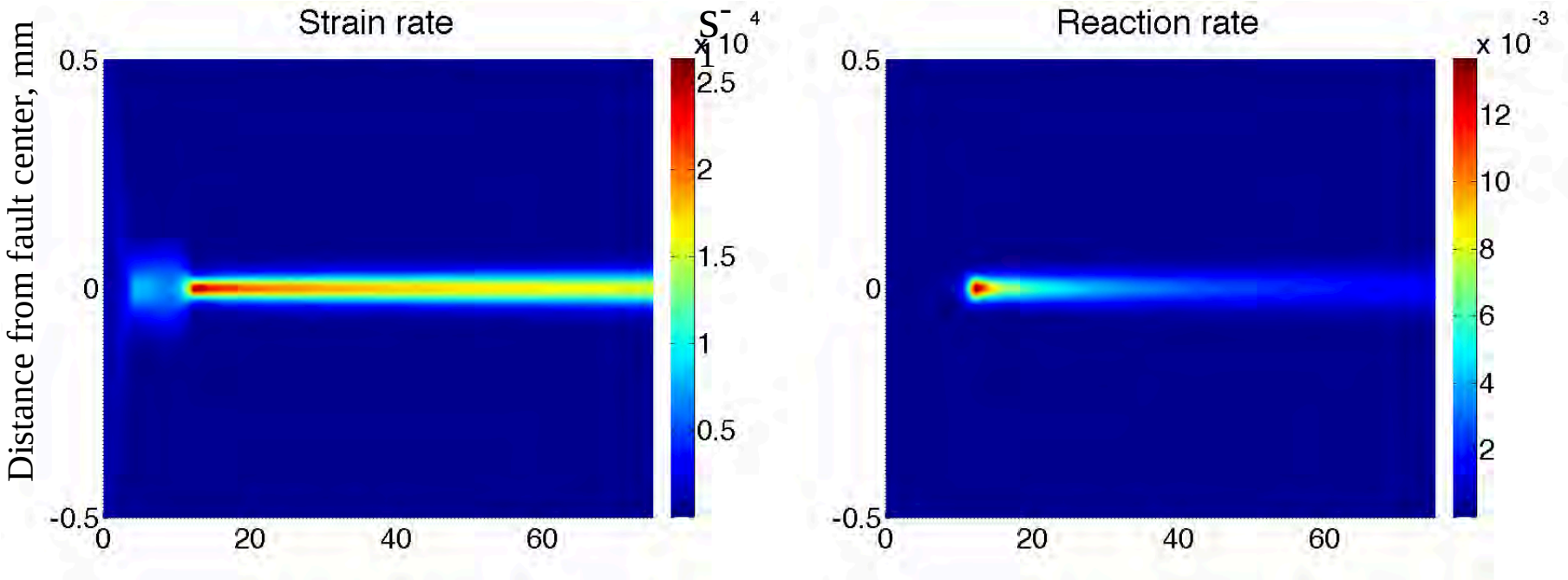


•The localized zone width has only decreased by a factor of two.

Platt, Brantut & Rice (*AGU*, Fall 2011; *JGR* 2015)

# Localized zone migration

- Now we investigate a case for which **depletion of reactant** is important.

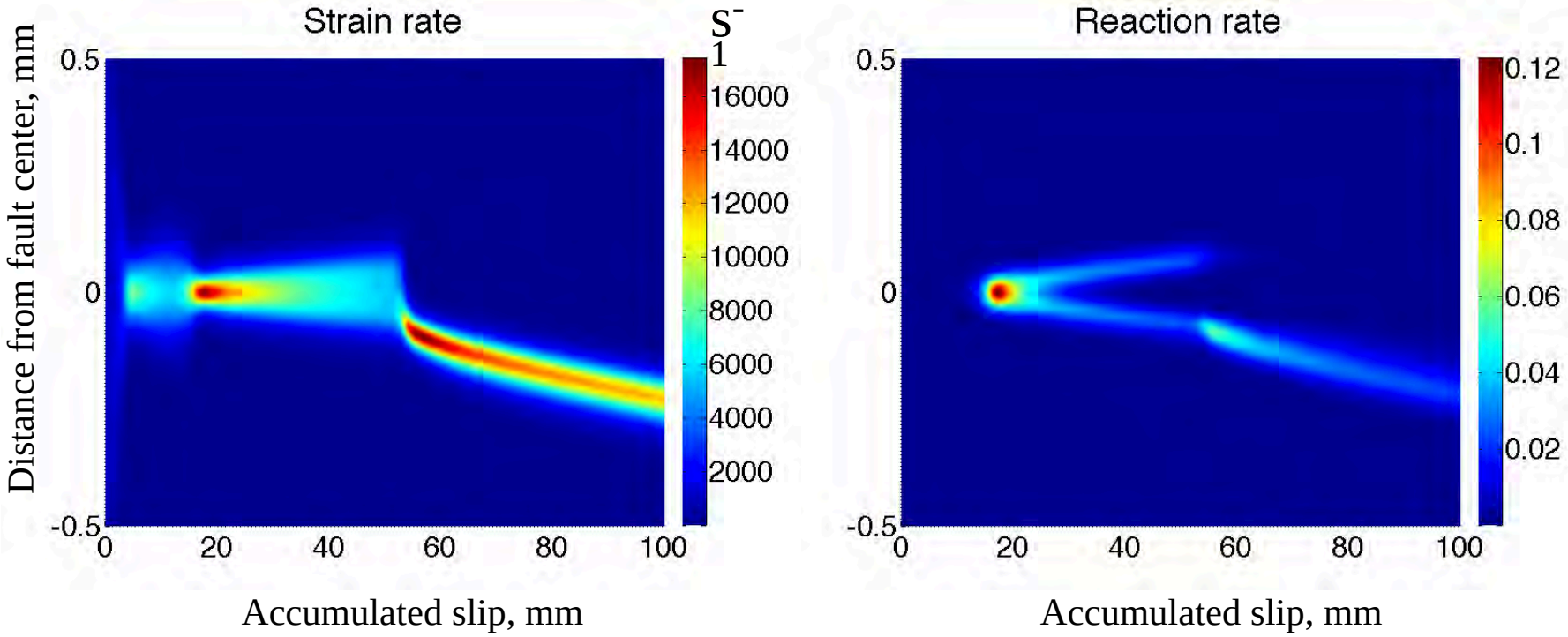


- Depletion causes the zone of localized straining to migrate. The strain rate and reaction rate profiles are strongly coupled.

Platt, Brantut & Rice (*AGU*, Fall 2011; *JGR* 2015)

# Localized zone migration

• This localized zone migration leads to a complex, non-monotonic, strain history.

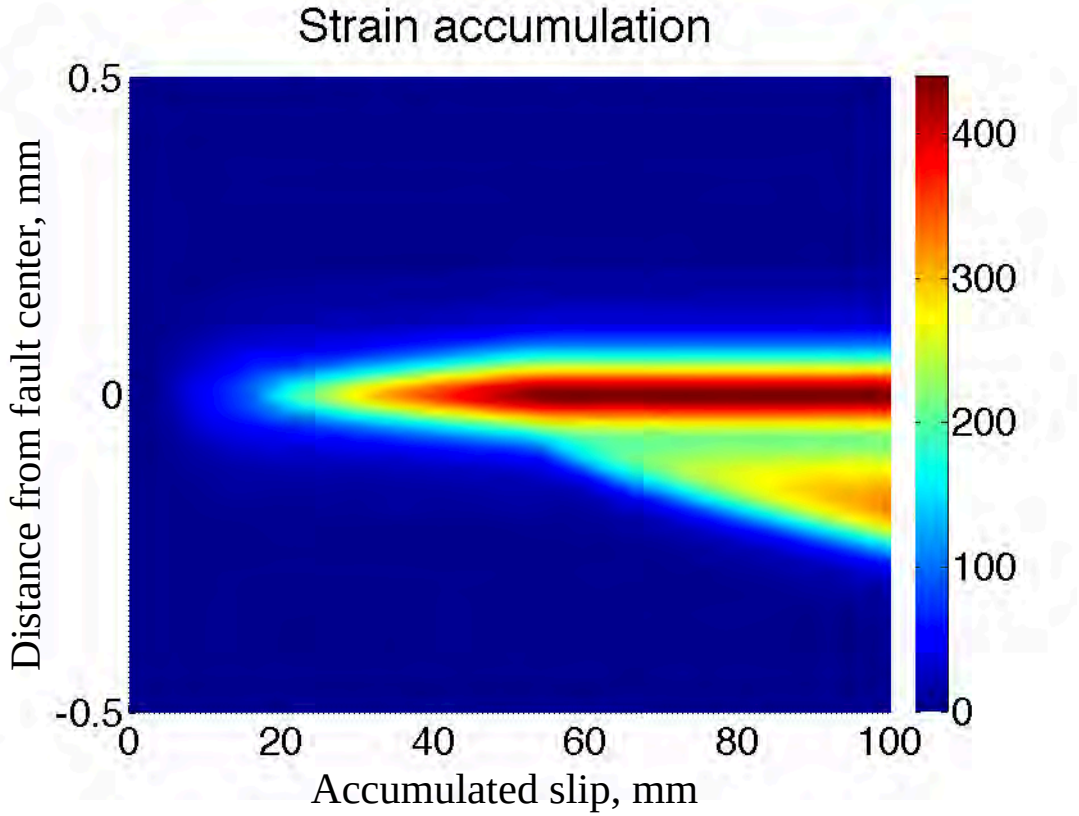


• Possible end result: Laminations in gouge.

Platt, Brantut & Rice (*AGU*, Fall 2011; *JGR* 2015)

# Observation suggesting migration (in rotary shear of carbonate sample)

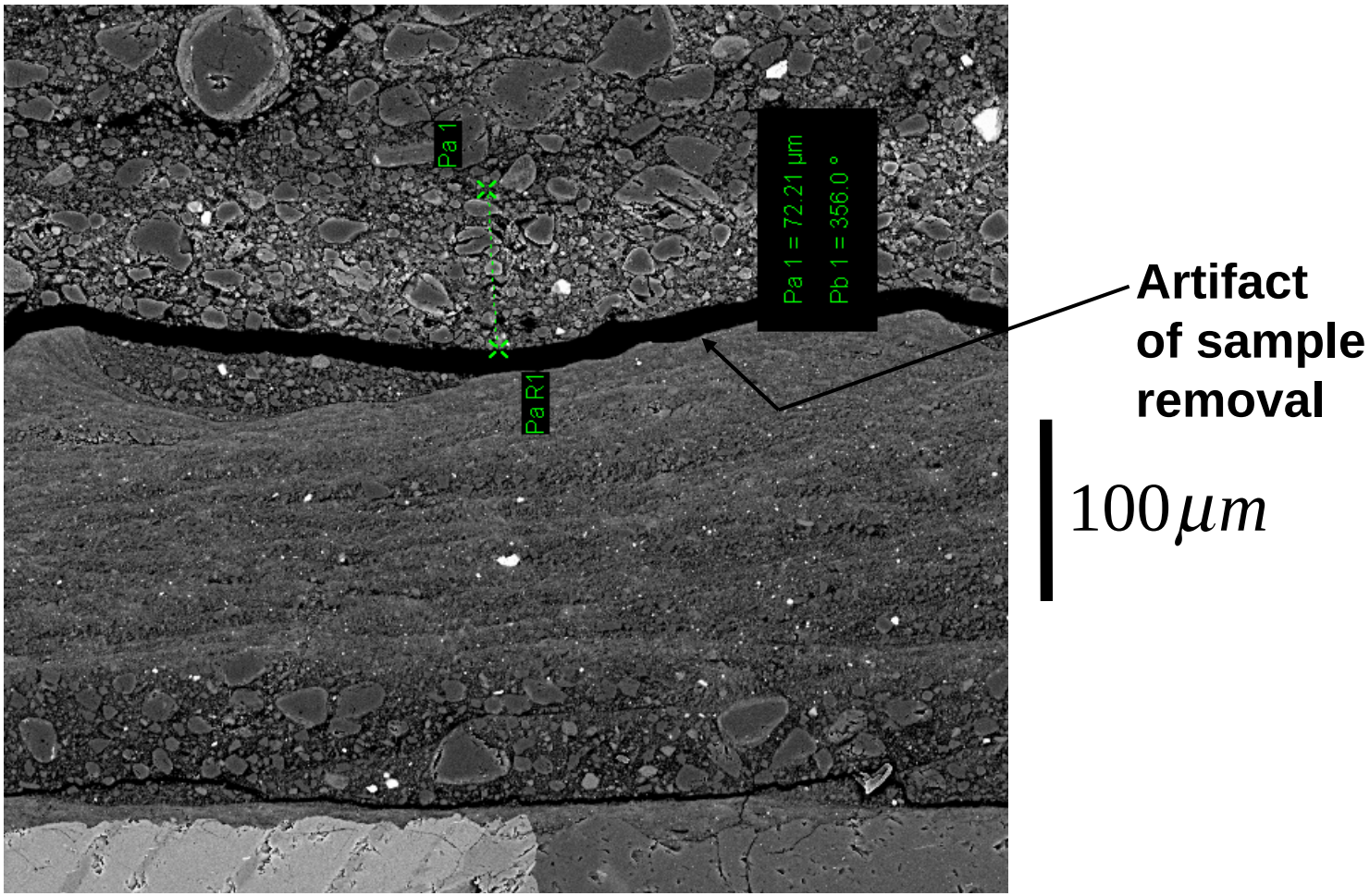


from T. Mitchell, Univ. Col. London (*private comm.*)

**• Another *weakening process expected to be important from start of seismic slip:***

**- Flash heating of asperity contacts, reduces *f* in rapid slip.**

**Most studied so far for bare surfaces in contact; recent extensions to fault gouge**

# *Flash heating of microscopic frictional asperity contacts*

[Rice, *AGU* 1999; *JGR* 2006; Beeler and Tullis, *AGU* 2003, Beeler et al. *JGR* 2008, building on Bowden and Thomas, 1954; Archard, 1958/59; Ettles,1986; Lim and Ashby, 1987.]

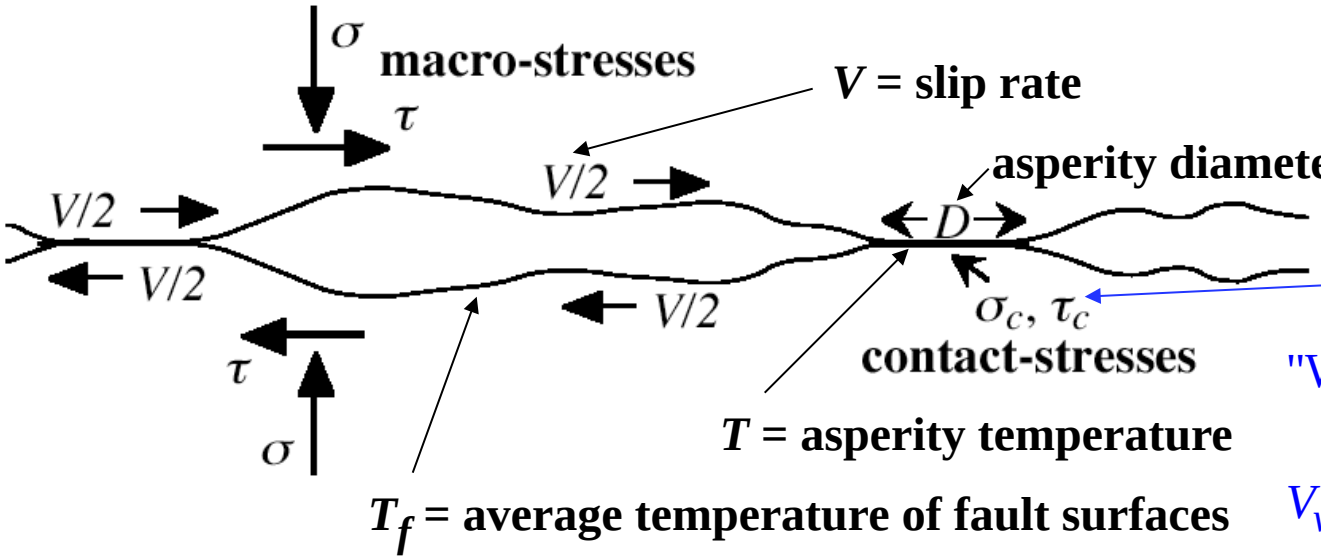


~ 0.1 μ

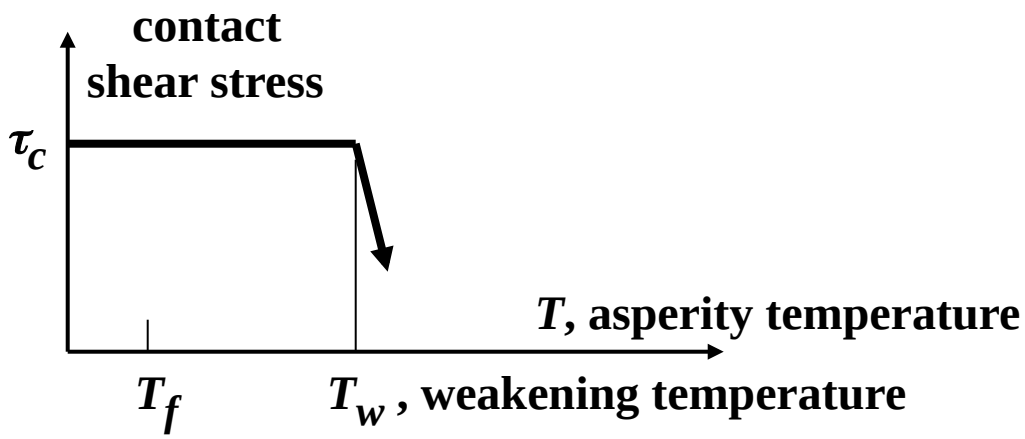


"Weakening" slip rate:

$$V_w = \pi \frac{\alpha_{th}}{D}\left(\frac{T_w - T_f}{\tau_c/\rho c}\right)^2$$

When $V > V_w$, asperity is weak for some of its life; suggests friction coef

$$f \approx f_{slow}\frac{V_w}{V} + f_{weak}\left(1 - \frac{V_w}{V}\right)$$

$$= f_{weak} + (f_{slow} - f_{weak})\frac{V_w}{V}$$

when $V > V_w$.

[Tullis & Goldsby, *SCEC*, 2003; *EOS*, 2003]

***Arkansas novaculite*** **(**~100% ***quartzite)***

Rotary Shear Apparatus

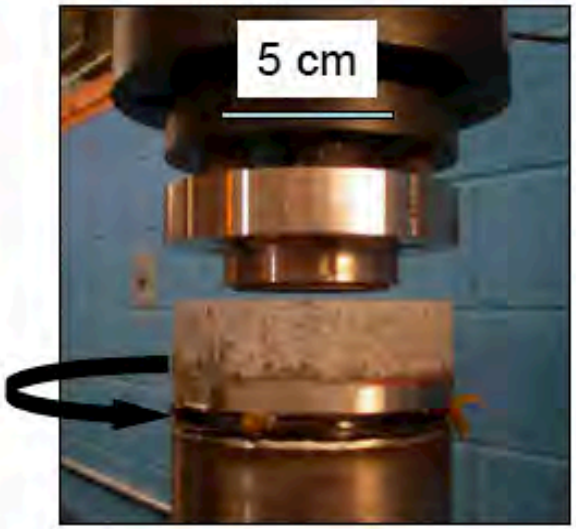


High speed $V \leq 0.36$ m/s

$\sigma_n = 5$ MPa

Rotary shear, 1.2 mm pre-slip at ~10 μm/s, followed by rapid slip for remaining 43 mm.

At low $V$, $f \approx 0.65$

At $V > 0.3$ m/s, $f \approx 0.30$

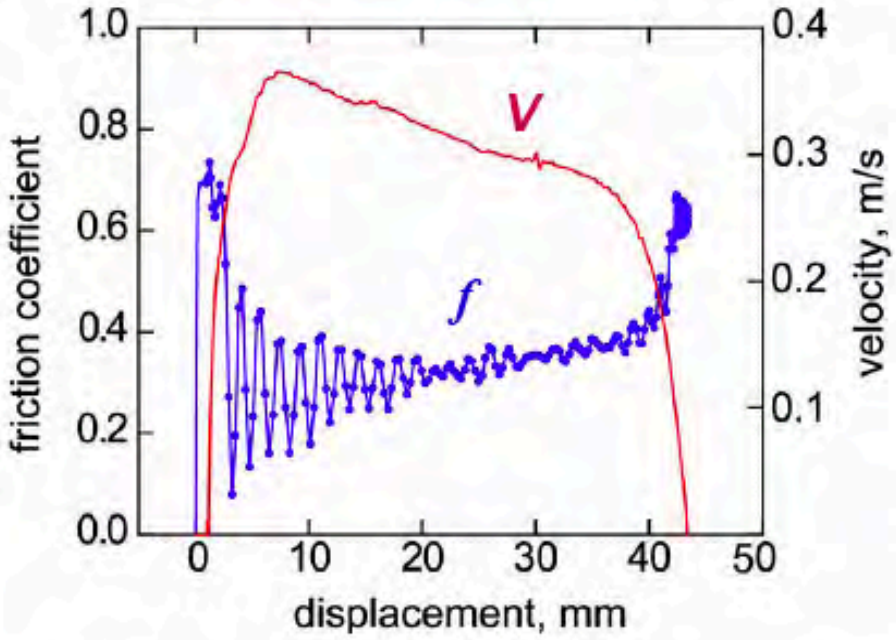


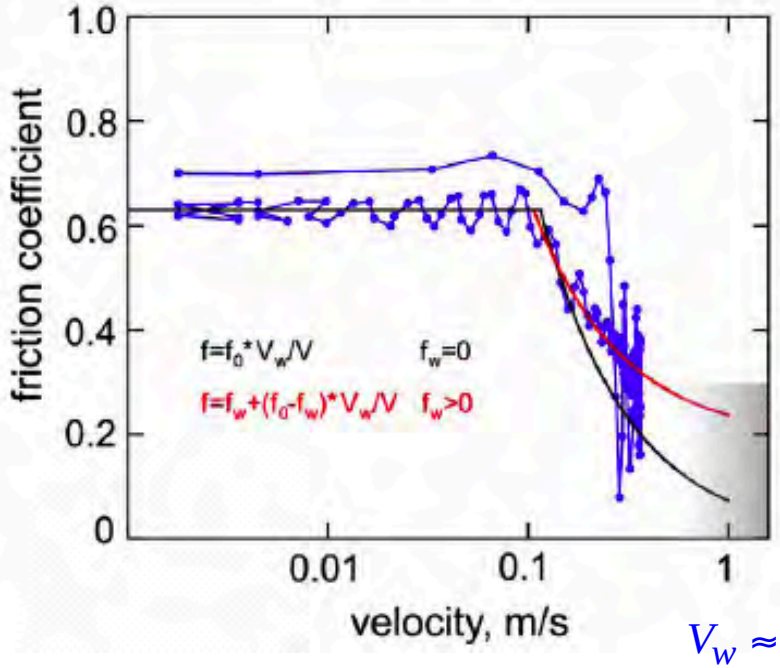


$V_w \approx 0.14$ m/s

## *Torsional Kolsky bar apparatus*

[Yuan & Prakash, *Int. J. Solids & Structures*, 2008]

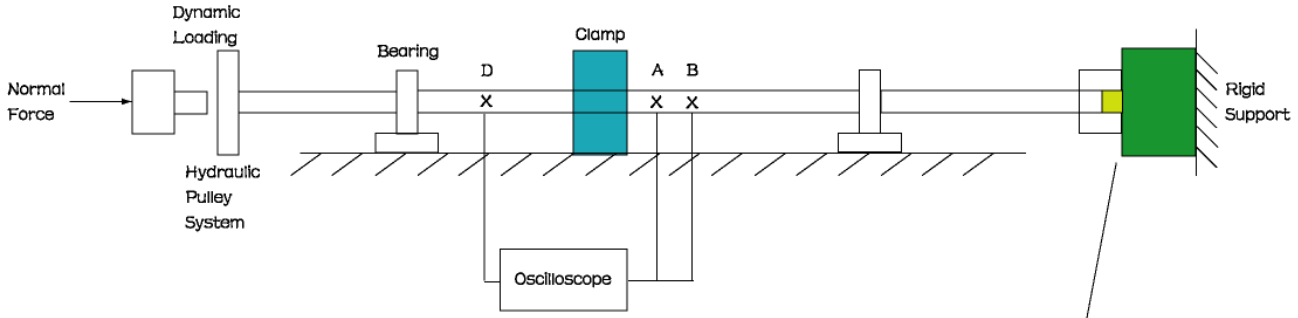


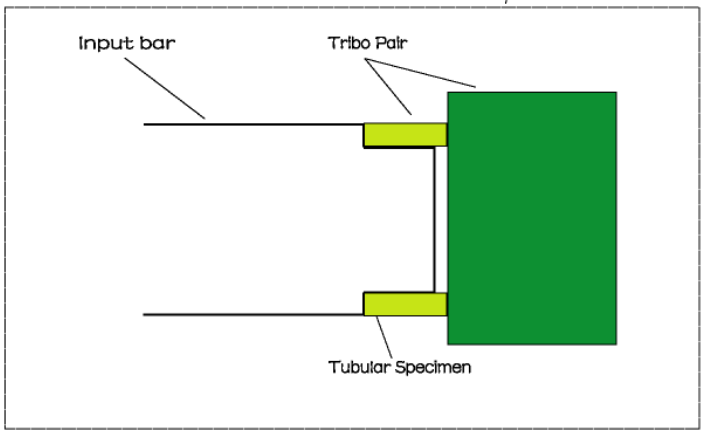


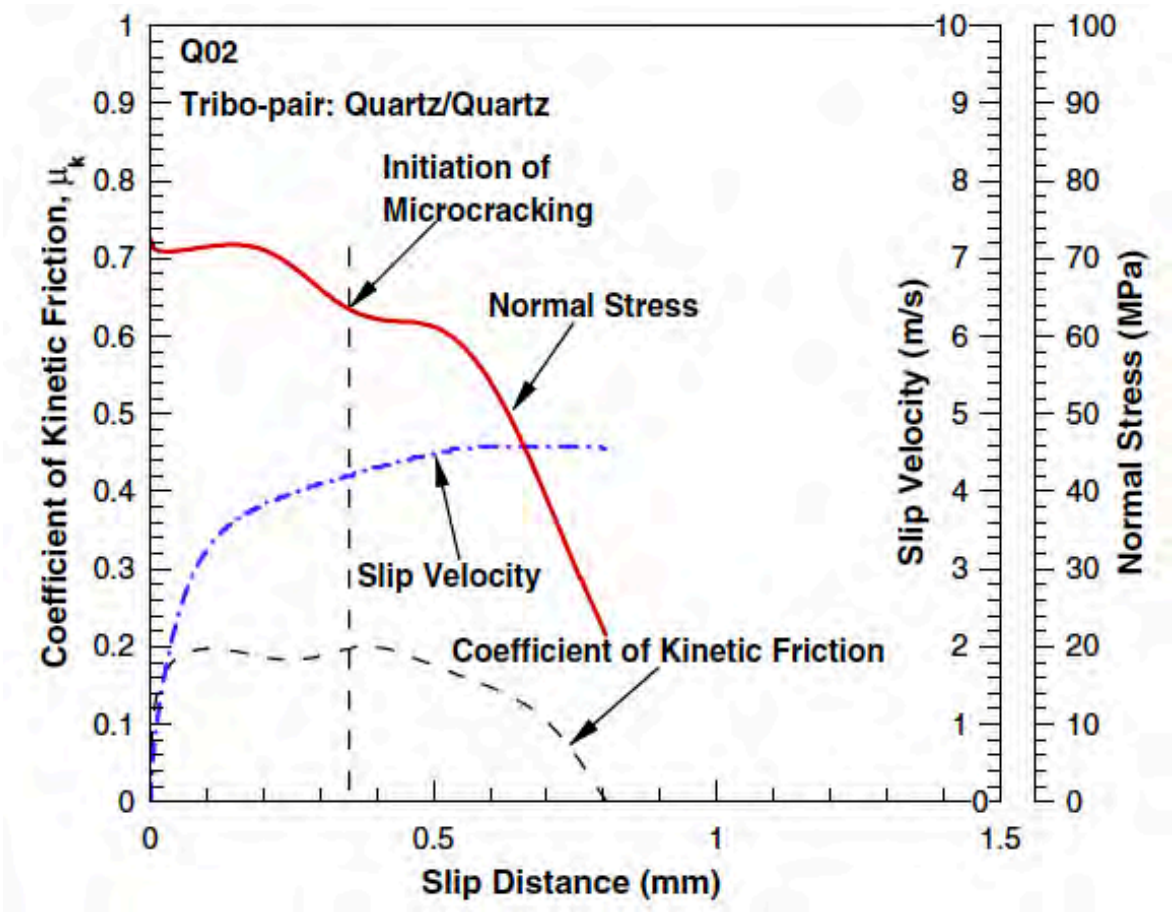


***Arkansas novaculite (quartzite)***

(Experiment becomes uninterpretable after small slip, marked, due to cracking in wall of specimen.)

Slip at $V \approx$ 2-4 m/s, resulting in $f \approx 0.20$.

## Goldsby & Tullis [Sci., 2011]:

### Test of simple flash weakening model,

$$f = f_o \text{ for } V < V_w \;,\; f = f_w + (f_o - f_w)\, V_w / V \text{ for } V > V_w$$

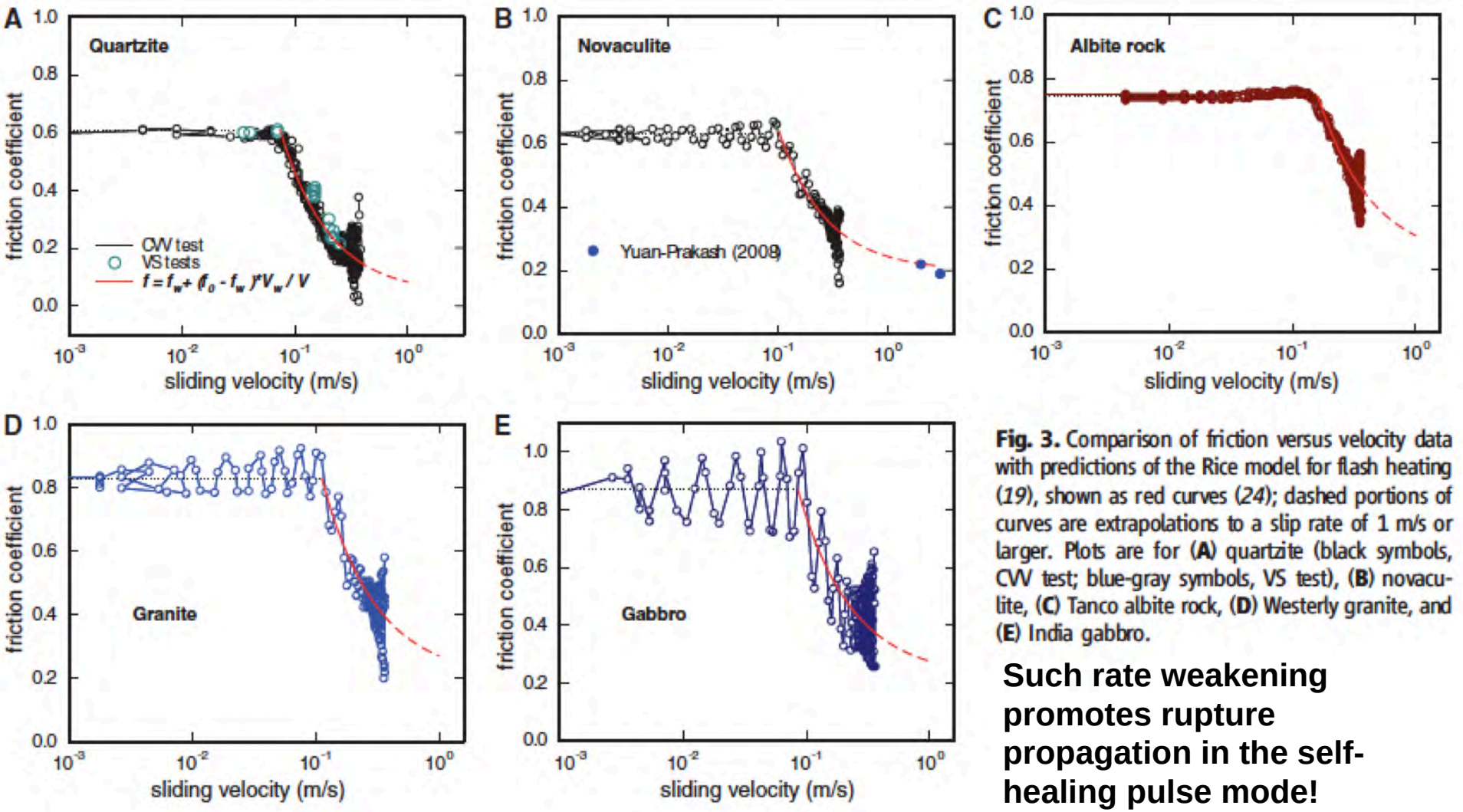


**Fig. 3.** Comparison of friction versus velocity data with predictions of the Rice model for flash heating (*19*), shown as red curves (*24*); dashed portions of curves are extrapolations to a slip rate of 1 m/s or larger. Plots are for (**A**) quartzite (black symbols, CVV test; blue-gray symbols, VS test), (**B**) novaculite, (**C**) Tanco albite rock, (**D**) Westerly granite, and (**E**) India gabbro.

**Such rate weakening promotes rupture propagation in the self-healing pulse mode!**

**Flash heating and weakening in gouge?**

**Some relevant studies:**

Beeler, N., T. E. Tullis, and D. L. Goldsby (JGR, 2008): **Constitutive relationships and physical basis of fault strength due to flash heating**

A. H. Kohli, D. L. Goldsby, G. Hirth, and T. E. Tullis (JGR, 2011): **Flash weakening of serpentinite at near‐seismic slip rates**

B. P. Proctor, T. M. Mitchell, G. Hirth, D. L. Goldsby, F. Zorzi, J. D. Platt, and G. Di Toro (JGR, 2014): **Dynamic weakening of serpentinite gouges and bare surfaces at seismic slip rates**

J. D. Platt, B. P. Proctor, T. M. Mitchell, G. Hirth, D. L. Goldsby, G. Di Toro, N. M. Beeler, and T. E. Tullis (AGU Abstr., 2014): **The role of gouge and temperature on flash heating and its hysteresis**

J. D. Platt, B. P. Proctor, T. M. Mitchell, G. Hirth, D. L. Goldsby, G. Di Toro, N. M. Beeler, and T. E. Tullis (AGU Abstr., 2014): **The role of gouge and temperature on flash heating and its hysteresis**

**Major points:**

**Building on *Beeler et al.* [2008], total slip rate assumed to be shared between multiple frictional contacts.**

**Solving for the contact temperatures, flash heating occurs when the strain rate exceeds a critical rate. For a deforming zone 100 microns wide, $V_w$ is ~4 m/s (vs. ~0.1 m/s for bare surfaces) → flash heating much less efficient in gouge than for bare surfaces.**

**The lower contact slip rate → longer contact lifetimes → wider thermal boundary layer thickness *W* at contact**

**When $W \approx D$ (spacing between contacts) flash heating begins at much lower slip rates, and friction decreases slowly as the slip rate increases.**

**Hysteresis commonly seen in bare surface experiments, with higher friction observed during acceleration than deceleration. Accounting for the sensitive dependence of $V_w$ on sliding surface temperature $T_f$ allows to match some data for both acceleration and deceleration over a wide range of slip rates.**

# *Some Consequences for Earthquake Dynamics*

***Dynamic rupture simulations, incorporating flash heating of asperity contacts and thermal pressurization of pore fluid, with parameters constrained (to the extent possible) by laboratory observations***

[Noda, Dunham & Rice, *JGR* 2009]

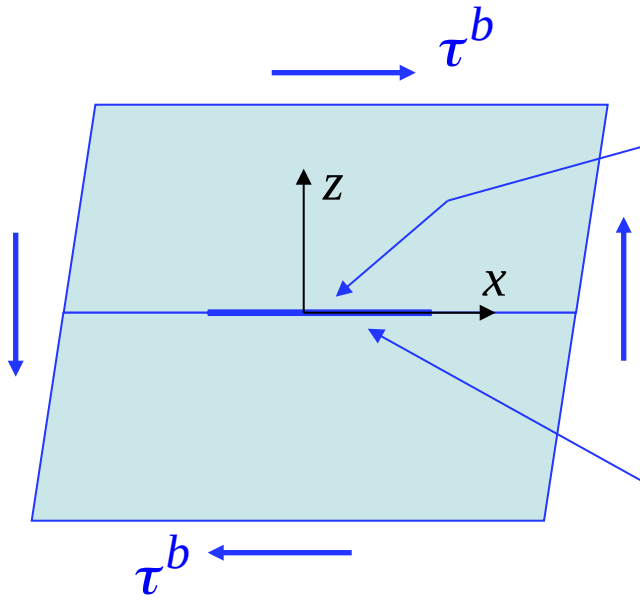


Rupture nucleated (by local overstressing) on fault under uniform background shear stress

$$\tau = \sigma_e f = (\sigma_n - p|_{z=0}) f$$

# *Flash heating* *(in dynamic rupture simulations, Noda, Dunham & Rice, JGR 09)*

**Effective stress law:**

*given, fixed compressive normal stress*

$$\tau = \sigma_e f = (\sigma_n - p|_{z=0})\, f$$

***friction coefficient***

*pore pressure on slip surface*

**Rate and state friction concepts, together with flash heating at microscopic contacts during rapid slip:**

$$\frac{df}{dt} = \frac{a}{V}\frac{dV}{dt} - \frac{V}{L}\left[ f - f_{ss}(V) \right]$$

- $$f_{ss}(V) = \begin{cases} f_{LV}(V), & V \le V_w, \\ f_w + \left( f_{LV}(V) - f_w \right)\dfrac{V_w}{V}, & V \ge V_w, \end{cases}$$

with $$V_w = \pi \frac{\alpha_{th}}{D}\left( \frac{T_w - T}{\tau_c / \rho c} \right)^2 ;$$

- $$f_{LV}(V) = f_o + (a-b)\ln\left( \frac{V}{V_o} \right)$$

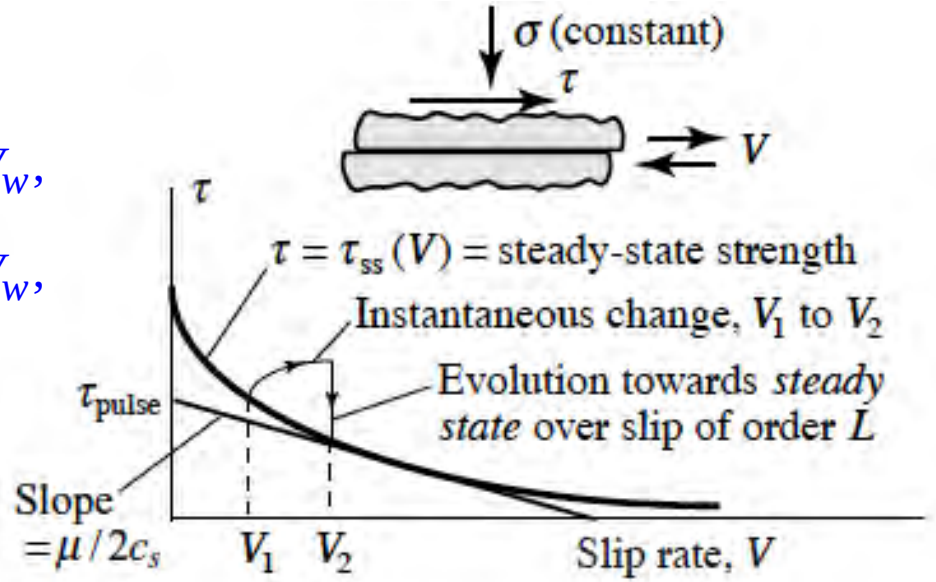

[Noda, Dunham & Rice, *JGR* `09]

**Based on Tullis and Goldsby [SCEC, `03] parameters $f_o$, $f_w$ and $V_w$ for granite.**

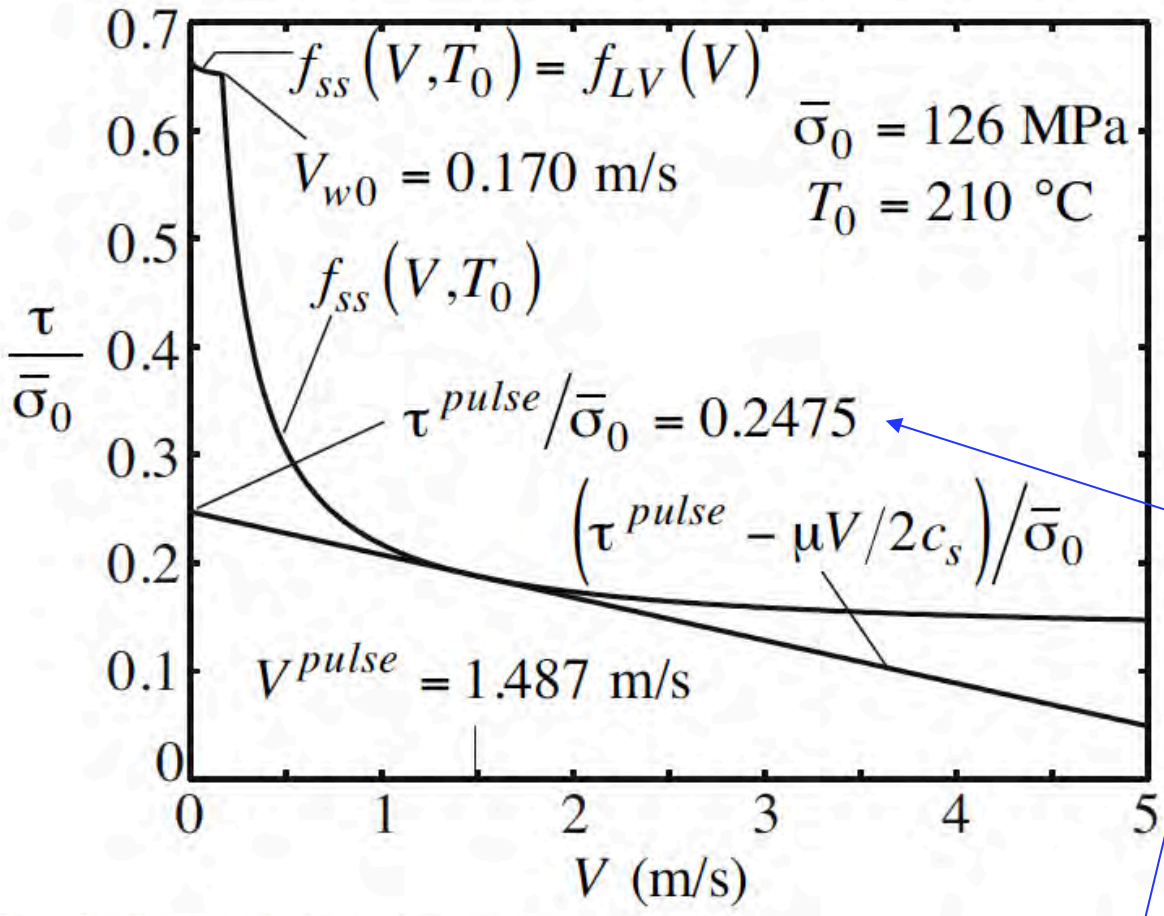


**Figure 1.** Steady state frictional shear stress, $\tau_{ss}$, normalized by initial effective normal stress, $\bar{\sigma}_0$, as a function of slip velocity, $V$. $\tau^{pulse}$ is defined for the initial ambient conditions at 7 km depth ($T = 210$ °C, $\sigma = 196$ MPa, $p = 70$ MPa) by the radiation-damping line which fits tangentially to $\tau_{ss}(V)$ at $V = V^{pulse}$ ($= 1.487$ m/s). The weakening slip rate is $V_w = 0.170$ m/s. Due to extreme velocity weakening at elevated slip rates, $\tau^{pulse}$ is very small ($0.2475\ \bar{\sigma}_0$).

Based on Zheng & Rice (BSSA, 1999), sustained rupture propagation expected to be possible, once nucleated, for background stress

$$\tau^b > \tau^{pulse} \approx 0.25\bar{\sigma}_0$$

***Thermal pressurization*** ***(in dynamic rupture simulations, Noda, Dunham & Rice, JGR 09)***

**Effective stress law:**

$$\tau = \sigma_e f = (\sigma_n - p|_{z=0})\, f$$

*given, fixed compressive normal stress*

*friction coefficient*

***pore pressure on slip surface***

**Thermal pressurization,** finite thickness of slipping zone, with Gaussian shear distribution having *r.m.s.* width *w*:

Conservation of energy (first law of thermodynamics):

$$\frac{\partial T}{\partial t} = \alpha_{th} \frac{\partial^2 T}{\partial z^2} + \frac{\tau}{\rho c} \frac{V}{\sqrt{2\pi}\, w} \exp\left( - \frac{z^2}{2w^2} \right)$$

Conservation of fluid mass (neglecting dilatancy):

$$\frac{\partial p}{\partial t} = \alpha_{hy} \frac{\partial^2 p}{\partial z^2} + \Lambda \frac{\partial T}{\partial t}$$

$\alpha_{th}$ ~ 0.7 mm$^2$/s; $\alpha_{hy}$ ~ 0.9 - 6 mm$^2$/s at mid-seismogenic depths; $\rho c$ ~ 2.7 MJ/m$^3$K; $\Lambda$ ~ 0.3 - 1.0 MJ/m$^3$K (Rice [*JGR* 2006] & Rempel & Rice [*ibid*], based on Wibberley [*EPS* 2002, *priv comm* 2003] & Wibberley & Shimamoto [*JSG* 2003], and estimates of damage)

[Noda, Dunham & Rice, *2008*; work preliminary to *JGR 2009*]

# Effect of hydrothermal properties

$\tau^{per}$ = 30MPa
$D^{per}$ = 5cm

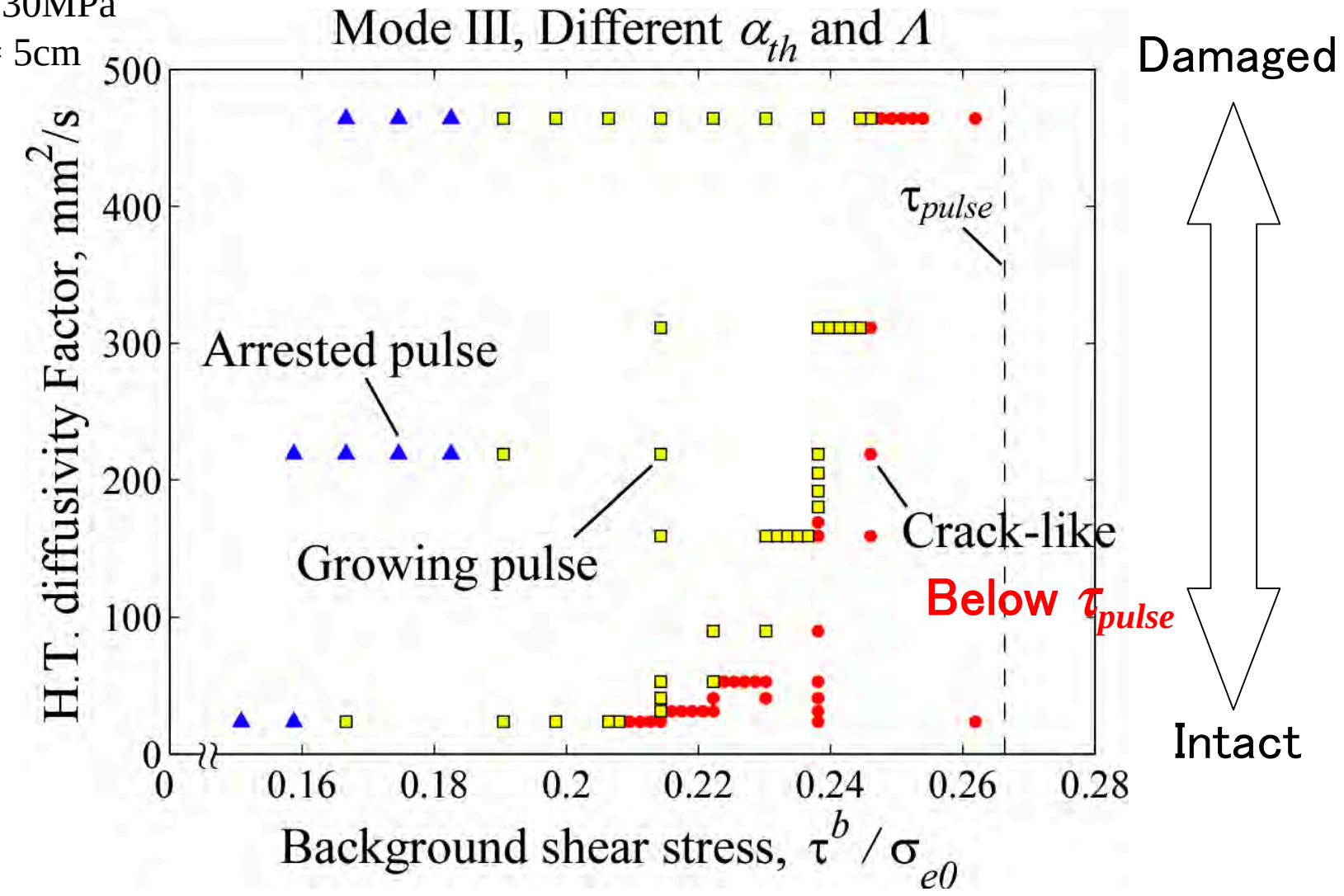


*Shown:*
The case $w = 0$, slip on a plane.

High $\tau^b$ favors crack-like solution, thermal pressurization does too.

[Noda, Dunham & Rice, *2008*; work preliminary to *JGR 2009*]

# Effect of hydrothermal properties

$\tau^{per}$ = 30MPa
$D^{per}$ = 5cm

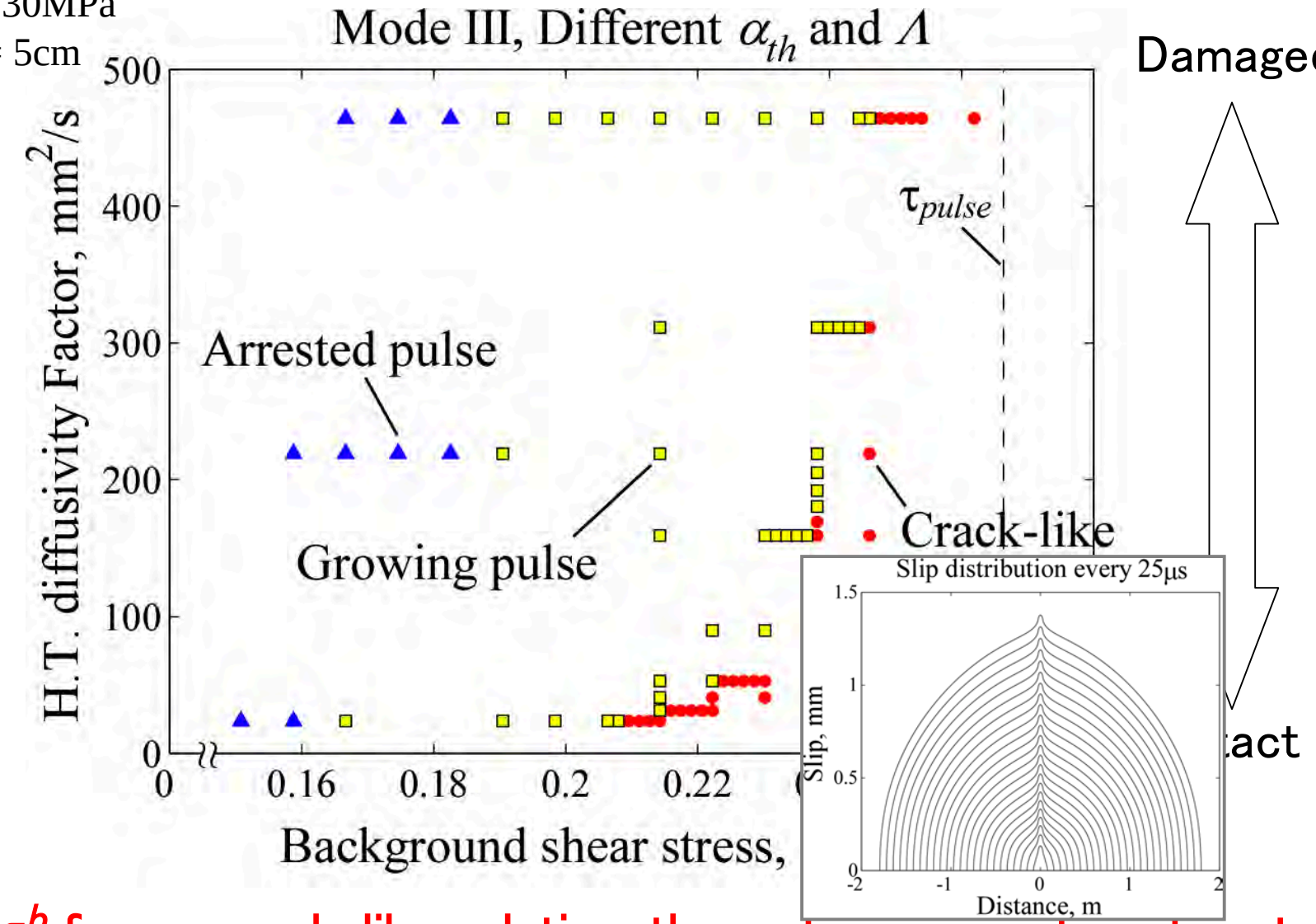


*Shown:*
The case $w = 0$, slip on a plane.

**High $\tau^b$ favors crack-like solution, thermal pressurization does too.**

[Noda, Dunham & Rice, *2008*; work preliminary to *JGR 2009*]

# Effect of hydrothermal properties

$\tau^{per}$ = 30MPa
$D^{per}$ = 5cm

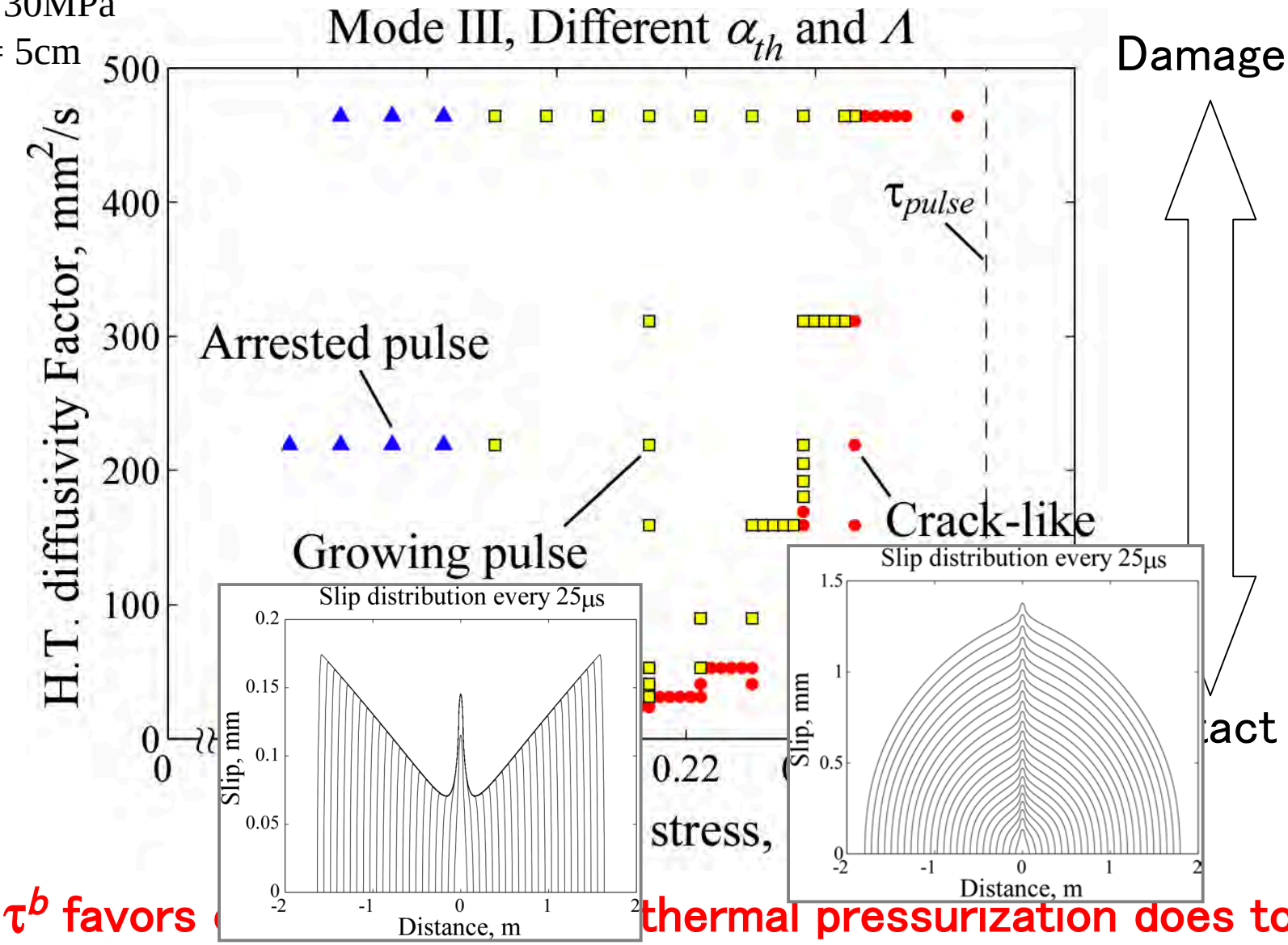


*Shown:*
The case $w = 0$, slip on a plane.

High $\tau^b$ favors ( thermal pressurization does too.

[Noda, Dunham & Rice, *2008*; work preliminary to *JGR 2009*]

# Effect of hydrothermal properties

$\tau^{per}$ = 30MPa
$D^{per}$ = 5cm

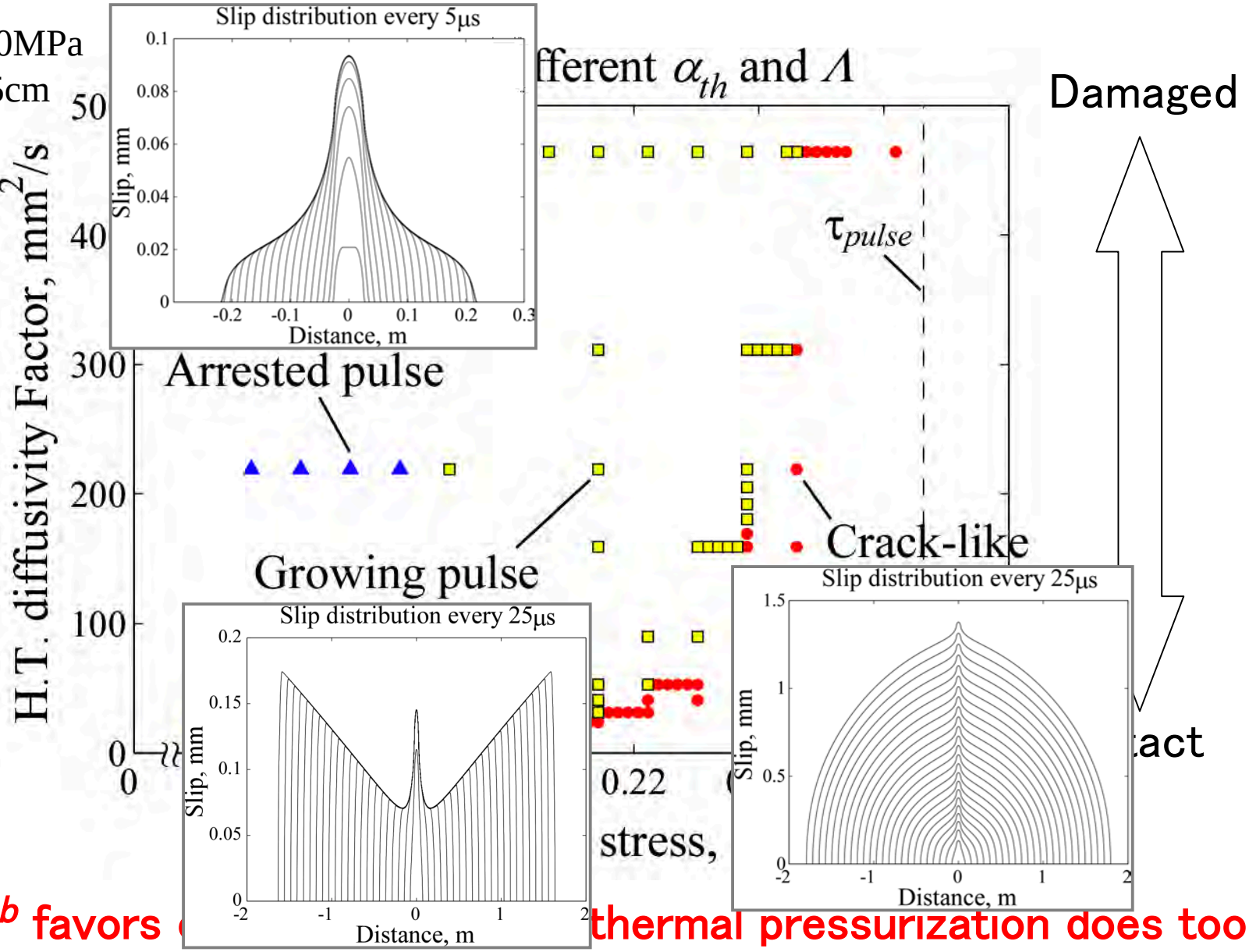


*Shown:*
The case $w = 0$, slip on a plane.

High $\tau^b$ favors ( thermal pressurization does too.

[Noda, Dunham & Rice, *2008*; work preliminary to *JGR 2009*]

# Effect of hydrothermal properties

$\tau^{per}$ = 30MPa
$D^{per}$ = 5cm

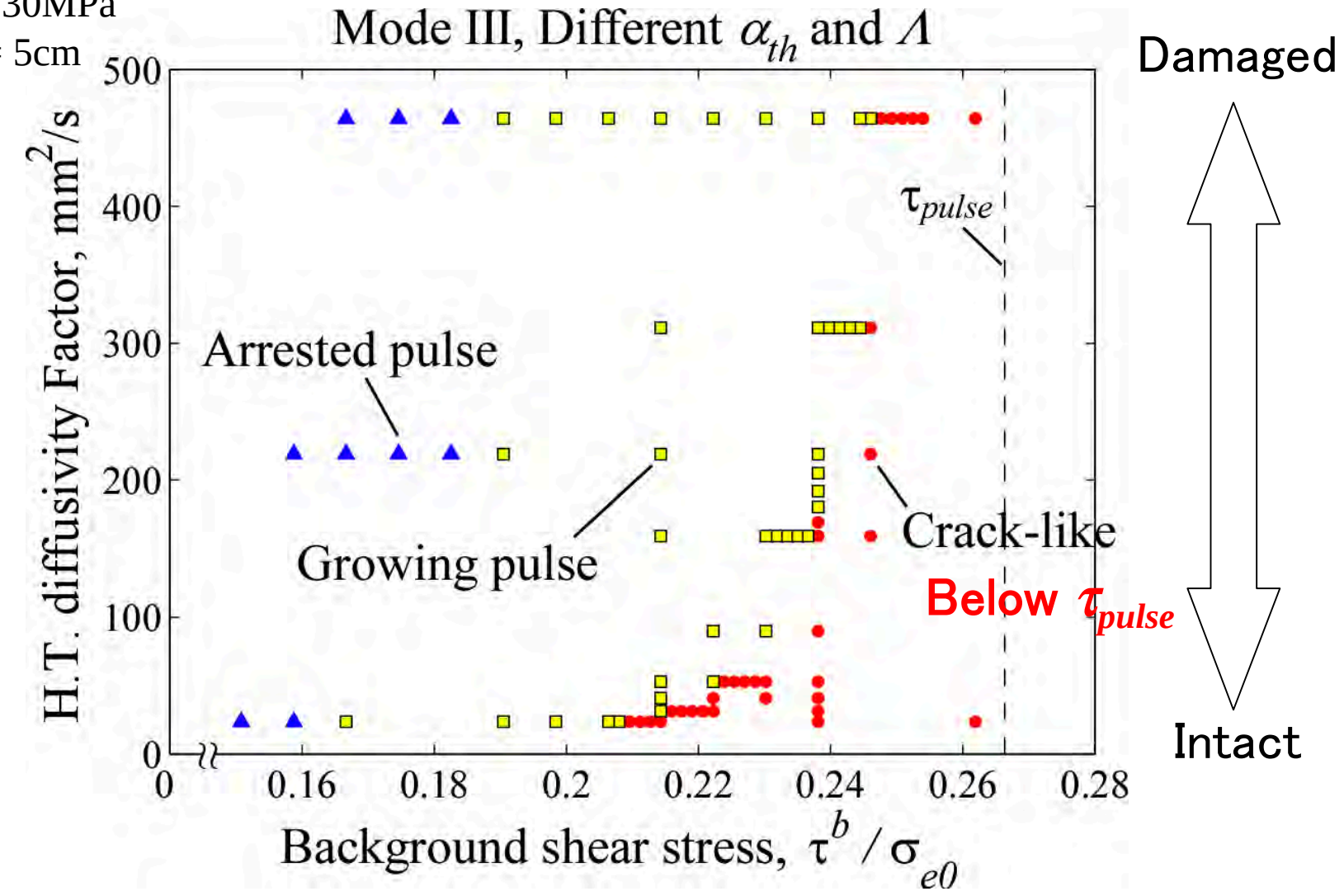


*Shown:*
The case $w = 0$, slip on a plane.

High $\tau^b$ favors crack-like solution, thermal pressurization does too.

Noda, Dunham & Rice [*JGR, 2009*]

# Comparing a growing slip pulse at $\tau^b = 0.230\,(\sigma_0 - p_0)$ to an enlarging shear crack at $\tau^b = 0.238\,(\sigma_0 - p_0)$

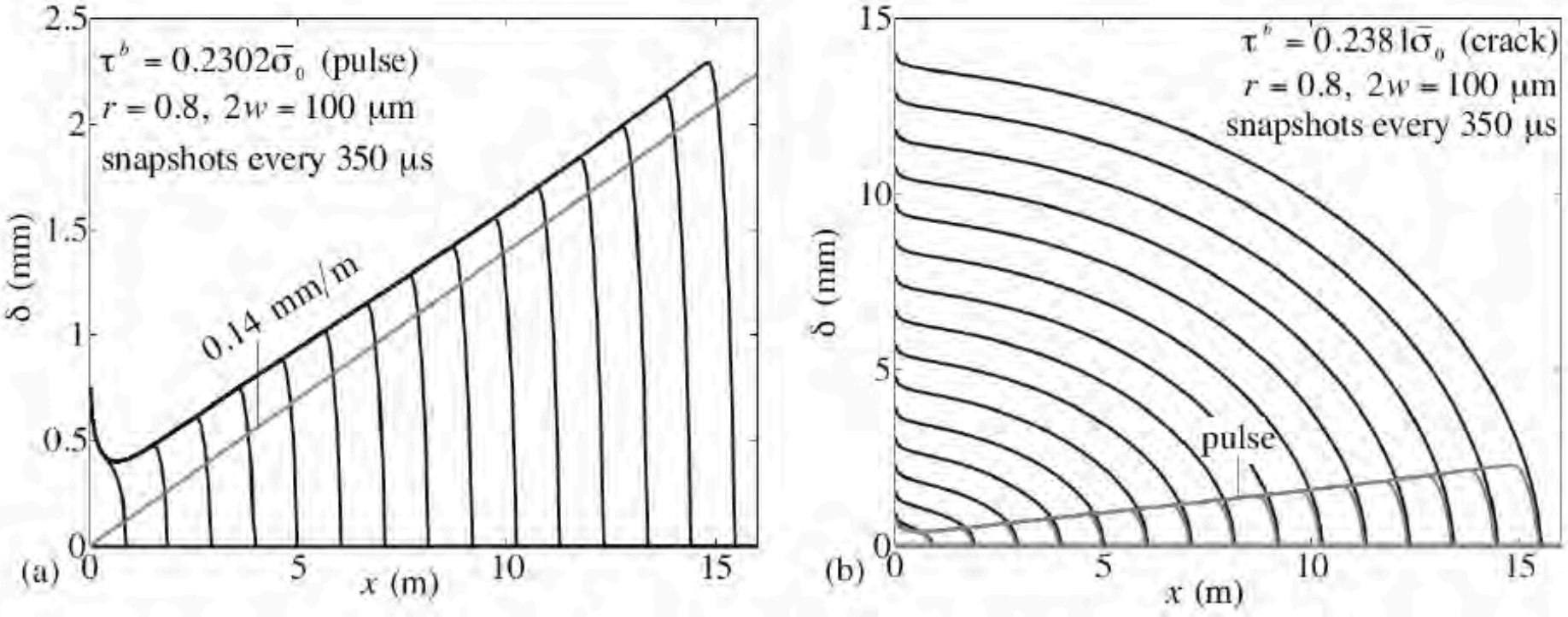


Both predict (if projected to circular fault) Seismic Moment $M_o$ [Nm] $\approx \lambda \times 10^{17} \left(t\ [\mathrm{s}]\right)^3$;

$\lambda \approx 1.7$ for ***slip pulse***, $\lambda \simeq 10.5$ for ***crack***; compare, $\lambda \approx 2$ for Parkfield 2004 [Uchide]

[Using $\delta^{3D}/\delta^{2D} = 0.73$, $\mu$=35 GPa, $\rho$=2800 kg/m$^3$ ( $c_s$ = 3.5 km/s ), and $v_r = 0.8 c_s$ ]

# Parkfield: San Andreas Fault Observatory at Depth

[Hickman & Zoback, *GRL* 2004]

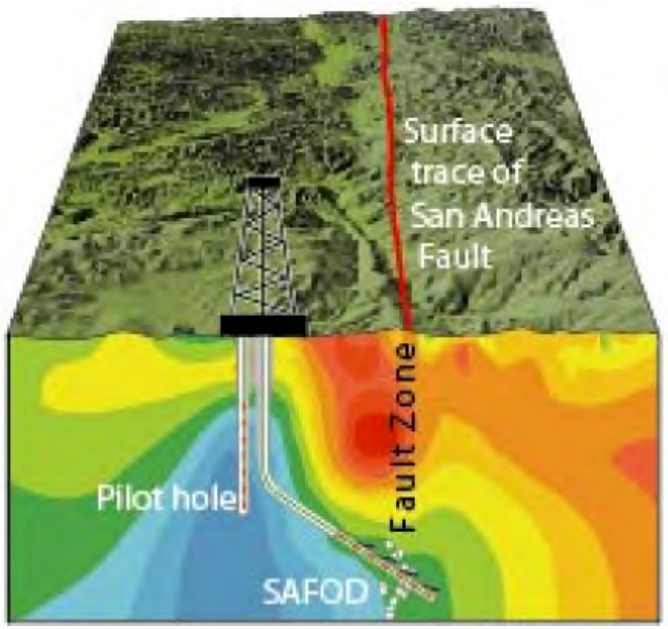


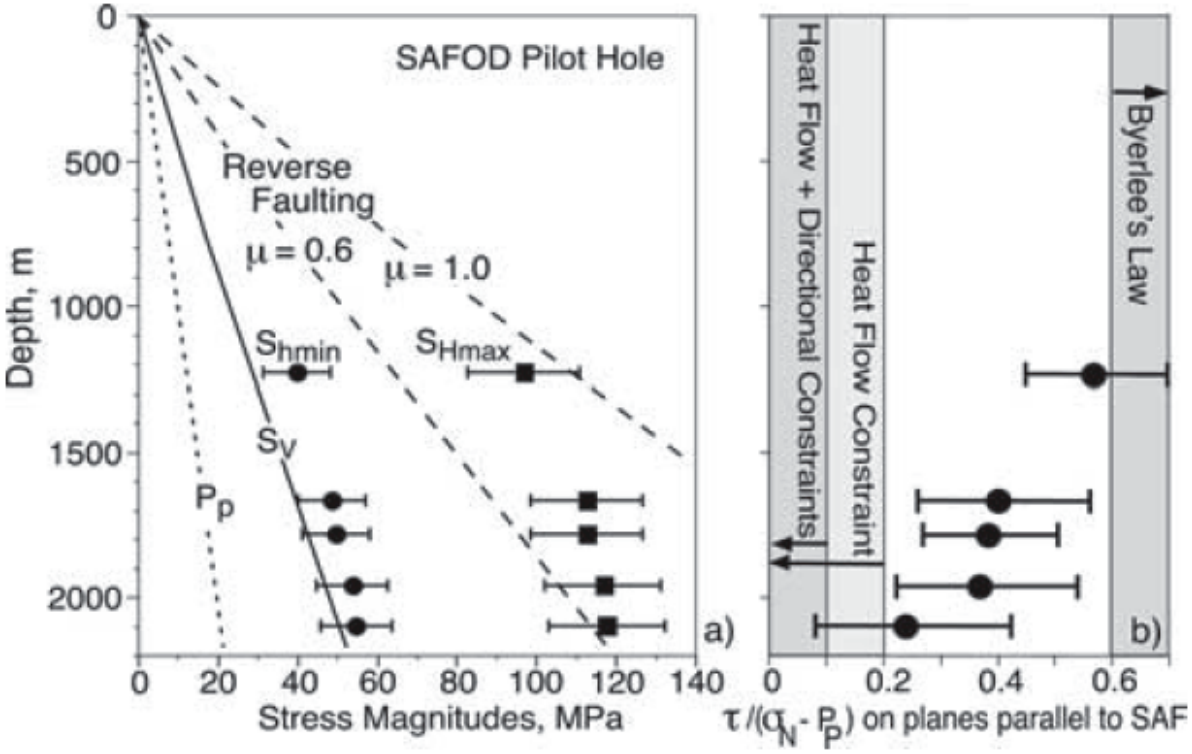


Simulations show growing pulse for ~ 0.22-0.24

**Steady-state pulse solutions, from Dmitry I. Garagash, *"Seismic and Aseismic Slip Pulses Driven by Thermal Pressurization of Pore Fluid"*, to *JGR*, 2012:**

***Assumes:*** • Friction coefficient $f$ = const.
• Shear zone thickness $W$ = const.

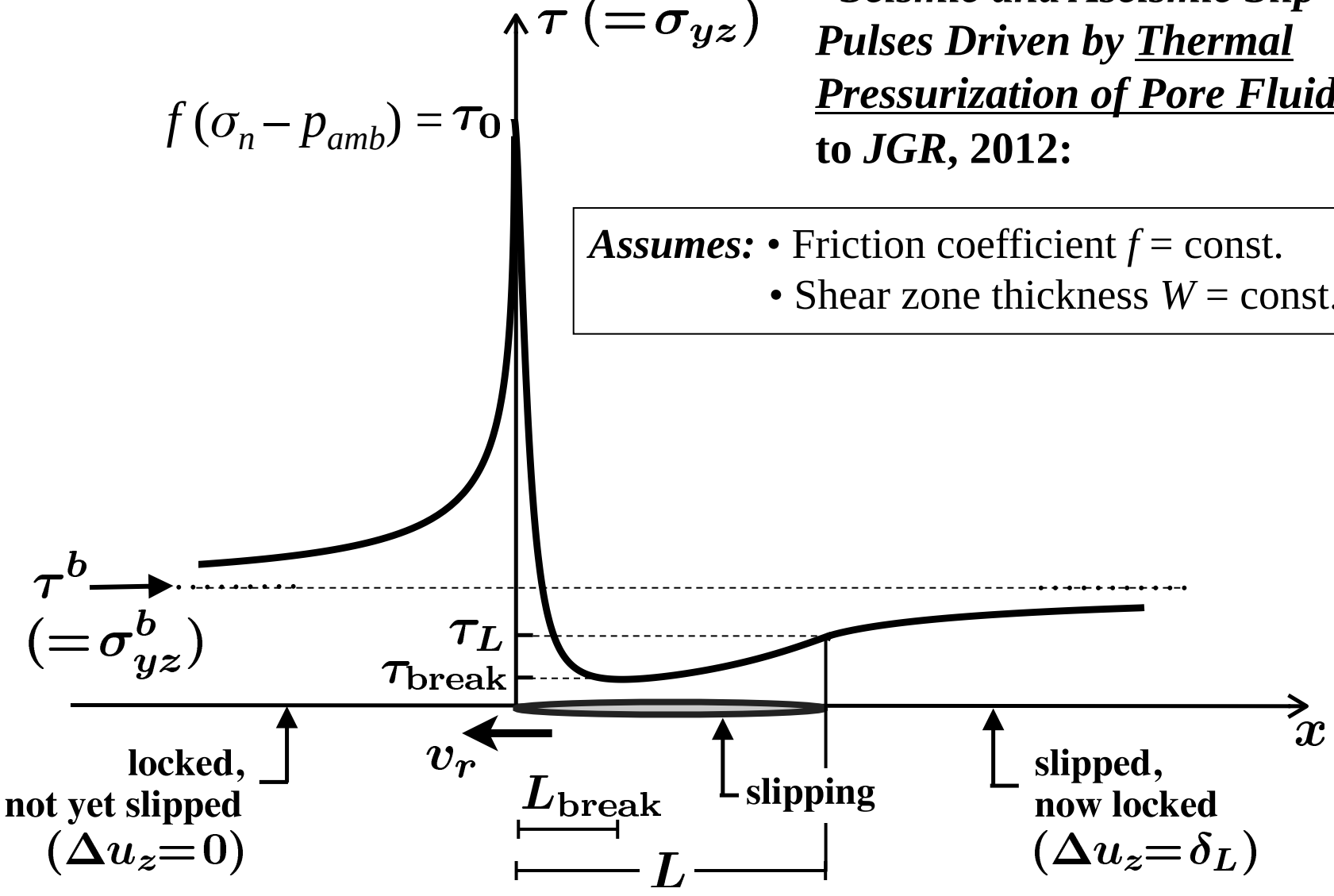

**Steady-state pulse solutions, from Dmitry I. Garagash, *"Seismic and Aseismic Slip Pulses Driven by Thermal Pressurization of Pore Fluid"*, *JGR*, 2012:**

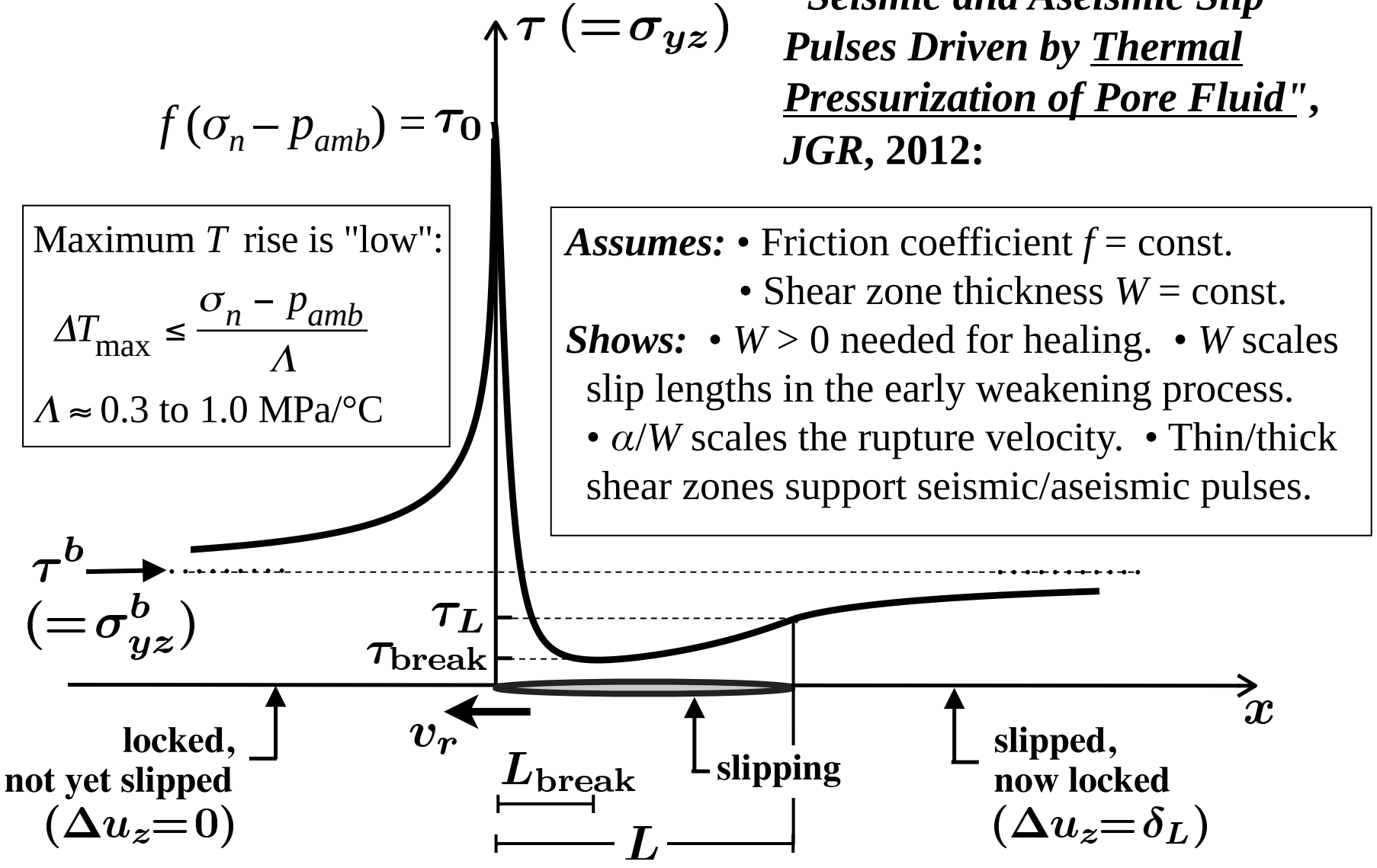


Maximum $T$ rise is "low":

$$\Delta T_{\max} \le \frac{\sigma_n - p_{amb}}{\Lambda}$$

$\Lambda \approx 0.3$ to 1.0 MPa/°C

***Assumes:*** • Friction coefficient $f$ = const.
• Shear zone thickness $W$ = const.

***Shows:*** • $W > 0$ needed for healing. • $W$ scales slip lengths in the early weakening process. • $\alpha/W$ scales the rupture velocity. • Thin/thick shear zones support seismic/aseismic pulses.

**Conclusions:**

- $\tau_{static}$ **much larger than** $\tau_{seismic}$.
- **Documented weakening (and localization) processes:**
  - **flash heating;**
  - **thermal pressurization, in-situ & decomp product;**
  - **nanoparticle-related ←(physics remains unclear);**
  - **melting.**
- **Static strength** $\tau_{static} = f_s \sigma_n$ **is unreliable predictor of pre-earthquake stress on major, well-slipped , smooth faults.**
- **Such faults may operate near or slightly above** $\tau_{pulse}$ **(a** $\tau$ **at which a small event, once nucleated, propagates indefinitely).**
- **Roughness may keep less mature faults from full benefit of dynamic weakening; to slip, side-walls must be deformed**
- **The fact that a segment is creeping does not preclude it from having large coseismic slip (Chi-Chi, 1999, Tohoku-Oki, 2011).**

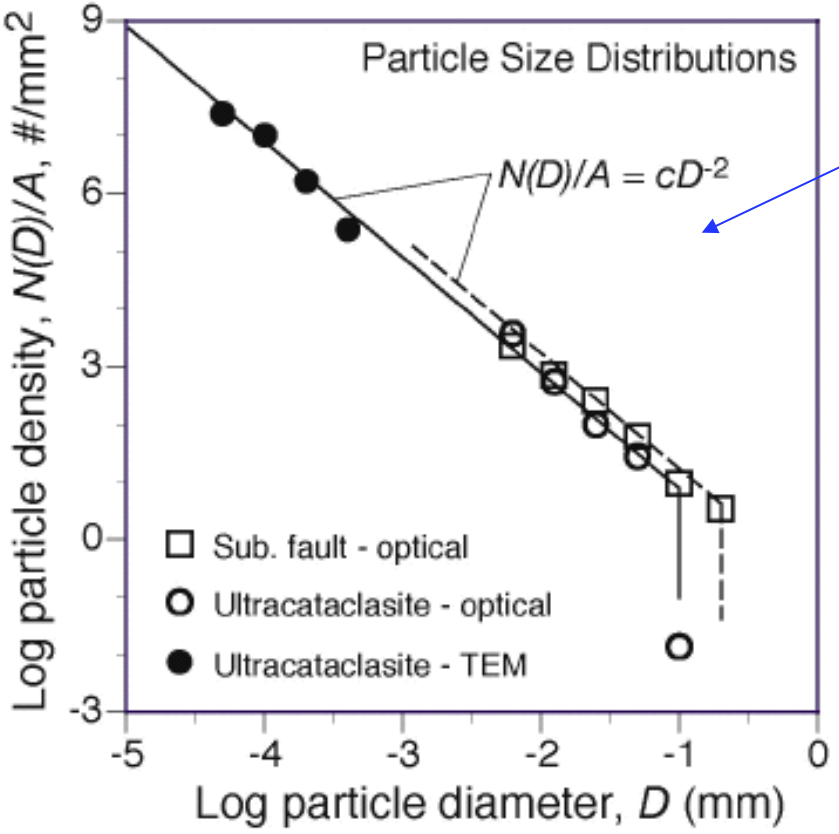


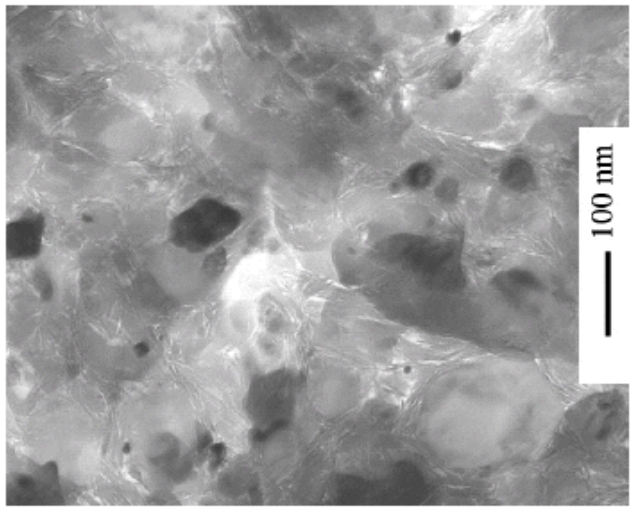


***Particle size distribution for Ultracataclasite gouge hosting the Punchbowl pss***
[Chester et al., *Nature*, 2005]

- $N(D)/A$ = number of particles per unit sample area with $2D/3 <$ diameter $< 4D/3$.

- $N(D)/A \approx c/D^2$ for 30 nm $< D <$ 70 μm.
In 3D: $\hat{N}(D)/V \approx \hat{c}/D^3$

- $D_{50}$ (= size such that 50% by mass are larger/smaller) ~ 1 μm.

- Standard granular material guideline (for narrow size range): thinnest possible shear zone ~5 to 10 $D_{50} \approx$ 5 to 10 μm